bnhcrc.com.au

bushfire&natural HAZARDSCRC

A MODIFIED SEVERE TROPICAL CYCLONE MARCIA (2015) SCENARIO: WIND AND STORM TIDE HAZARDS AND IMPACTS

Richard J. Krupar III and Matthew S. Mason
School of Civil Engineering, The University of Queensland
Bushfire and Natural Hazards CRC

THE UNIVERSITY OF QUEENSLAND
AUSTRALIA

RISK FRONTIERS

Version	Release history	Date
1.0	Initial release of document	19/7/2017

Australian Government
Department of Industry, Innovation and Science
Business Cooperative Research Centres Programme

Publisher:
Bushfire and Natural Hazards CRC

July 2017

Citation: Krupar III, R. J., and Mason, M. S. (2017) A modified Severe Tropical Cyclone Marcia (2015) scenario: wind and storm tide hazards and impacts. Bushfire and Natural Hazards CRC, Melbourne.

Cover: Cyclone wind damage during Tropical Cyclone Marcia in Queensland, February 2015.

TABLE OF CONTENTS

EXECUTIVE SUMMARY

This report describes research undertaken to develop a modified Severe Tropical Cyclone Marcia (2015) scenario and details its wind and storm tide-related impacts on buildings and society in Livingstone Shire and the Rockhampton Region. A perturbed version of the original track taken by Cyclone Marcia was chosen to create an ensemble event set of possible worst-case wind and storm tide inundation scenarios for the region of interest and the key findings of this work are as follows:

- Fifty storm scenarios were generated using modified 72 hr European Centre for Medium-range Weather Forecasting (ECMWF) ensemble storm track and intensity forecasts. Several scenarios caused widespread wind and storm tide-induced impacts.
- In Byfield, Rockhampton and Yeppoon, 90% of the simulated maximum site-relative three-second gust wind speeds were at or below 75 ms^{-1}, 59 ms^{-1} and 68 ms^{-1} respectively.
- At the 90^{th} percentile, roughly 43% of all residential homes experienced severe structural damage.
- The total number of inhabitable homes decreased for both pre- and post-1981 residential building construction with increasing percentile range.
- The maximum simulated storm tide for the entire ensemble event set was 5.83 m.
- Total loss ratios maxed out across the towns of Bangalee, Cooee Bay and Rosslyn for all percentile storm tide heights calculated for the entire ensemble event set. This led to many homes becoming inaccessible due to high flood waters.
- Both wind and storm tide impacts are highly sensitive to simulated storm parameters such as track and intensity, so the highest quality event information is needed if realistic impact results are to be generated.

Future work will seek to improve the exposure dataset used in this scenario. Improvements will include adding critical infrastructure such as power lines and water distribution networks, as well as, updating Geocoded – National Address File (G-NAF) building level estimates of property value, contents value and population using ground truth data. The wind, rainfall and storm surge hazard models and associated vulnerability models used in the current multi-hazard model framework will also be updated. The wind hazard model will include new environmental parameters (i.e. sea surface temperature and deep layer wind shear) that influence tropical cyclone formation and maintenance. This improvement will help generate more realistic cyclones wind fields. The rainfall hazard model will be calibrated to Australian surface terrain and topography to simulate inland rainfall enhancements and will be paired with a hydrodynamic runoff model to simulate inland flooding damage and impacts to buildings, critical infrastructure and society during the post-landfall phase. The storm tide hazard model will be updated to simulate inland flooding impacts (e.g. surge-induced riverine flooding) by including the influence of the underlying surface roughness overland and expanding the mesh inland. Updates to the wind and flood vulnerability models will be made as new results surface from Bushfire and Natural Hazard CRC projects aiming to develop and improve these types of models. The flood vulnerability model will be updated to include flow velocity and wave effects. Finally, combined or joint hazard impacts (i.e. wind driven rain) will be evaluated to develop joint-hazard damage functions in future model releases.

1 INTRODUCTION

Severe Tropical Cyclone Marcia (2015) was the southernmost category 5 cyclone to make landfall in Queensland since the advent of the reliable Bureau of Meteorology (BoM) historical tropical cyclone database. While storm surge impacts were minimal for this event given the storm's landfall trajectory, significant wind-related impacts to buildings in Byfield, Rockhampton and Yeppoon were observed. If the storm were to have shifted to the east by approximately 30 km, a completely different scenario would have unfolded for these towns, especially Yeppoon. There is a need to examine what wind and storm tide impacts could have occurred given a range of different scenarios (e.g. landfall locations both east and west of the original landfall location).

This report details the final scenario in a series of reports that are part of the Bushfire and Natural Hazards CRC project, "*Using realistic disaster scenario analysis to understand natural hazard impacts and emergency management requirements*." The 72 hr European Centre for Medium - range Forecasting (ECMWF) ensemble prediction forecast for Cyclone Marcia is modified and used to generate fifty possible wind and storm tide scenarios and their associated impacts on buildings and their occupants in Livingstone Shire Council and the Rockhampton Region. Thus far, only wind related impacts have been modelled and discussed in previous reports. This report is the first to model the storm tide hazard impacts on buildings and society.

The beginning of this report details the nature and impacts of Cyclone Marcia upon which this scenario is based, and describes how the scenario was created (section 2). Then, it details the underlying exposure (i.e. demographic, topography, etc.) information utilised, the multi-hazard model methodology implemented, including a brief description of the wind, rainfall and storm tide hazard models and the wind and flood vulnerability models (section 3). Following the description of the exposure data and the multi-hazard and vulnerability modelling framework are the scenario results with a focus on the range of possible wind and storm tide impacts on buildings and society across the study region (section 4). Localized damage and impacts in Byfield, Rockhampton and Yeppoon, Queensland, are examined in closer detail (when applicable). The report concludes with a summary of results and an outline for future research opportunities (section 5).

2 SCENARIO EVENT OVERVIEW

Cyclone Marcia crossed Shoalwater Bay around 08:00 am AEST on 20 February 2015 as a category 5 cyclone based on satellite estimates of storm intensity. As the cyclone weakened to category 4 status at landfall, category 3 winds were observed by a BoM automatic weather station (AWS) near Yeppoon (roughly 68 km from the landfall point). These winds caused structural damage to many homes and power lines in Byfield and Yeppoon. Evidence of beach erosion and storm surge damage was noted near Shoalwater Bay and between One Mile Beach and Farnborough Beach north of Yeppoon (BoM 2017). Fortunately, Yeppoon did not experience significant flood damage because the peak storm surge coincided with a falling tide (BoM 2017). As the cyclone continued to track south, the eye passed over Rockhampton, where category 2 winds and moderate structural damage to homes was observed. Marcia was downgraded to a tropical low in the early morning hours of 21 February and crossed the Sunshine Coast in the late afternoon.

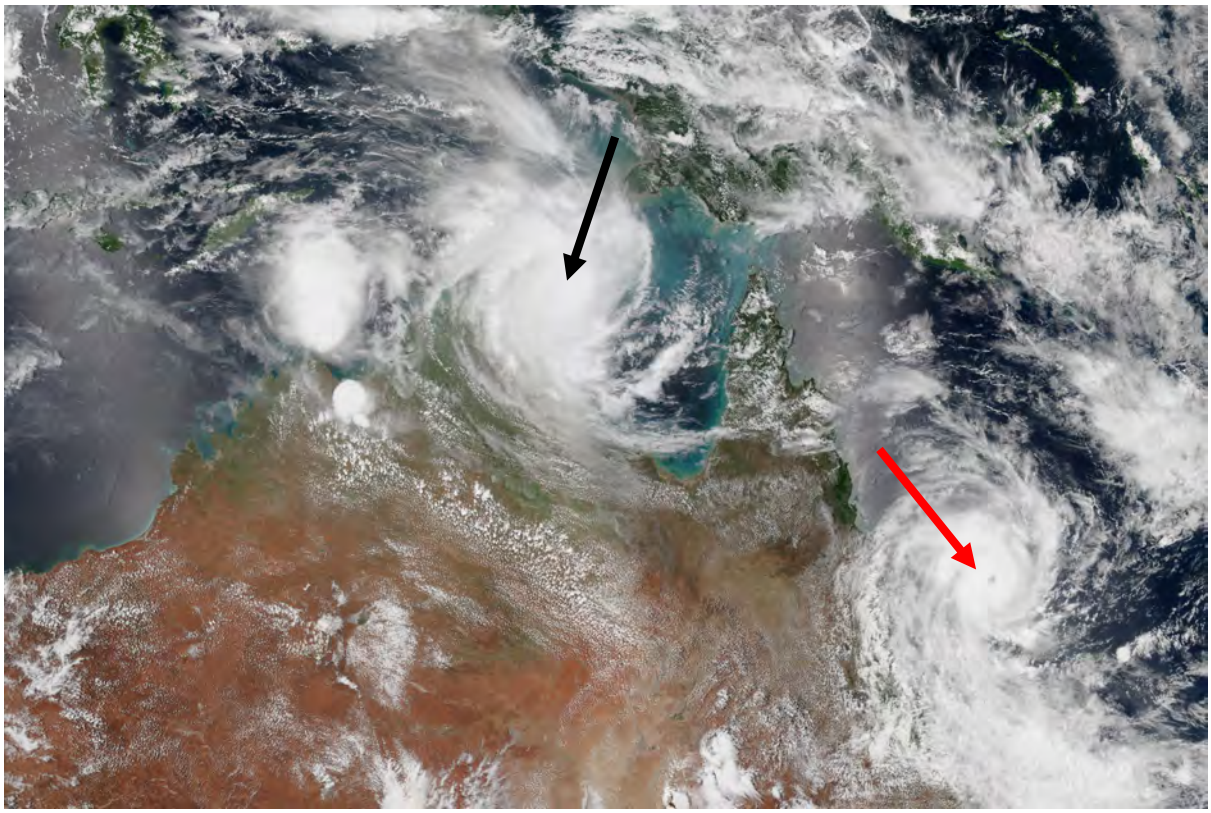

Figure 1. Satellite imagery for Tropical Cyclones Marcia (red arrow) and Lam (black arrow) in 2015 (photo courtesy of NASA, 2015).

A more precarious scenario for Livingstone Shire and the Rockhampton Region was generated by using the 72-hr ECMWF ensemble prediction system forecast starting on 17 February 2015 at 00 UTC (10:00 am AEST). This data was sourced from The International Grand Global Ensemble (TIGGE) National Centre for Atmospheric Research (NCAR) Research Data Archive. The goal of the TIGGE project is to provide researchers with a user interactive platform to vary ensemble predication system forecasts to accelerate improvements in high-impact weather forecasting. Thus, for this scenario, a single-track scenario was initially created using a slightly modified version of the 72 hr ECMWF ensemble mean storm track. This track was chosen because it was positioned well enough to the east of the original BoM best track to

generate a worst-case wind and storm tide scenario for the study region, especially for Yeppoon (e.g. the landfall location lies just to the east of Pearl Bay). By using the 72 hr ECMWF ensemble mean storm track, it allowed the eastern part of the storm to remain offshore and more water to pile up along the coast near Yeppoon as it moved inland. Slight modifications were necessary to allow stronger wind speeds to pass over Rockhampton than occurred in the original event (Figure 2). Once the storm cleared Rockhampton, it moved southeast and merged back with the original BoM best track, where the scenario was cut off at the 96 hr forecast point to focus the risk assessment on immediate landfall impacts. It should be noted that only the 72 hr ECMWF ensemble prediction system forecast was used in this study because the 48 hr and 24 hr ECMWF ensemble mean storm tracks came into better agreement with the original BoM best track and did not provide a comparable worst-case scenario for the study region.

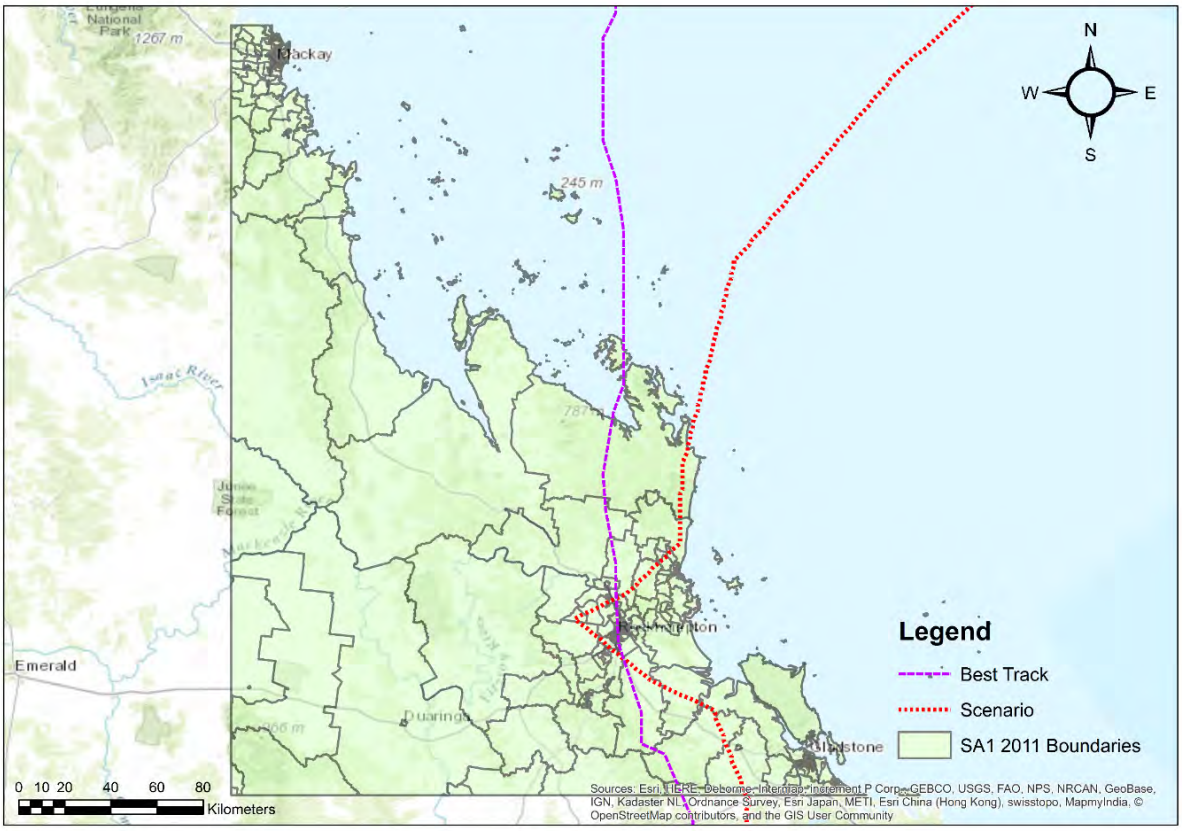

Figure 2. Best track and modified ECMWF ensemble mean storm track for Cyclone Marcia (2015).

Once the modified 72 hr ECMWF ensemble mean single track scenario had been created, each of the fifty ensemble forecasts generated by the ECMWF ensemble prediction system were shifted accordingly to match the position shifts applied to the ensemble mean storm track. The ECMWF ensembles represent perturbations from the original deterministic forecast generated by the numerical weather prediction model and were used to generate fifty potential landfall scenarios, rather than just one single track scenario. The shifted 72 hr ECMWF ensemble forecasts were also cut off at the 96 hr forecast point in this scenario to focus on immediate landfall impacts and are shown in Figure 3. It should be noted that the 72 hr ECMWF ensemble mean storm track was not used as a potential landfall scenario in this report, but rather to shift the entire ensemble event set to create more possible worse-case scenarios.

In the first report of this series (Mason 2015), it was mentioned that uncertainties around storm size and dynamics (e.g. eye wall replacements) make it exceedingly difficult to generate single, deterministic values for expected damage when operating in forecast mode. This is especially true for the Cyclone Marcia scenario, where the ECMWF failed miserably to forecast the rapid intensification phase that Marcia went through before making landfall. A storm intensity correction was required to generate an individual intensity forecast for the modified 72 hr ECMWF ensemble and ensemble mean storm tracks.

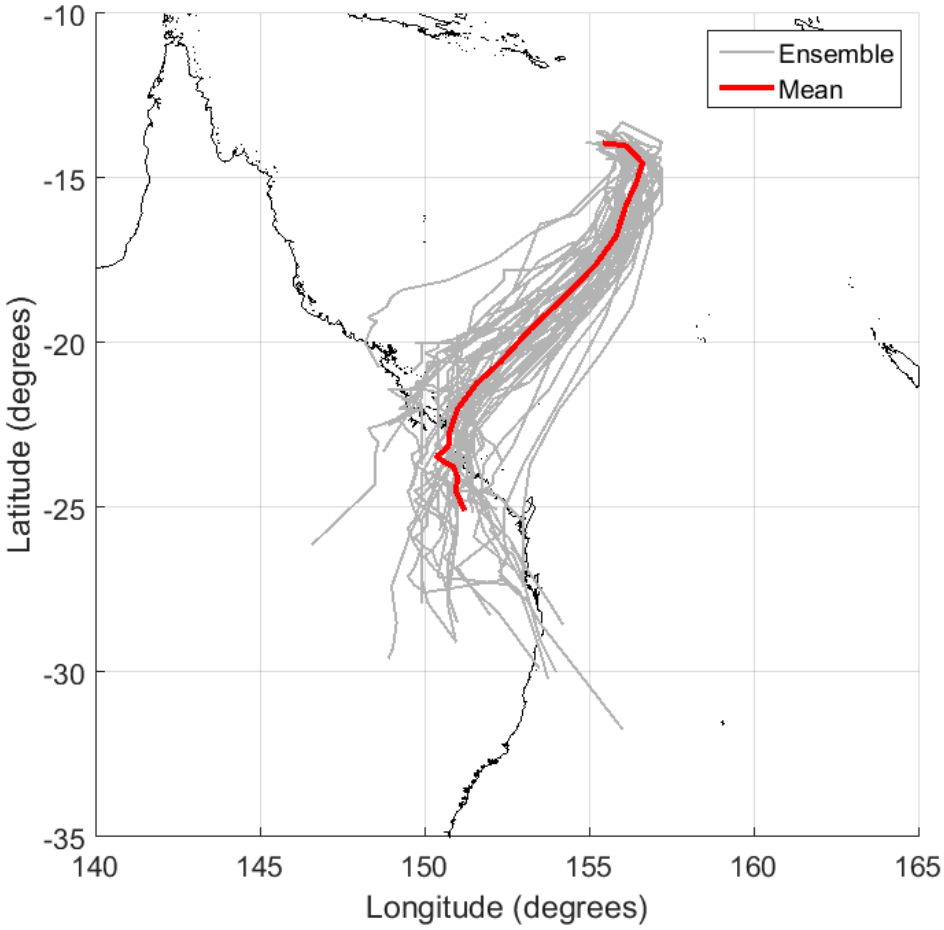

Figure 3. Modified 72 hr ECMWF ensemble and ensemble mean storm tracks used for the scenario.

For the single-track base scenario, the BoM best track minimum central pressure (C_p) values (Table 1) for the 96 hr simulation period were utilized to compute the Holland B parameter using the empirical relationship developed by Harper and Holland (1999). The Holland B parameter is a pressure shape parameter first developed by Holland (1980) to describe the relationship between surface pressure differences and maximum wind speeds, and generally describes the peakedness of the radial wind profile. The radius of maximum wind (RMW) and environmental or peripheral pressure (P_n) were also sourced from the BoM best track file to help define simulated wind fields. In the absence of RMW data (see Table 1), empirical estimates of RMW were computed using the empirical relationships developed by Vickery and Wadhera (2008). These parameters are often used to describe the size and intensity of tropical cyclones and were used as some of the inputs in the wind hazard model, which then fed into the rainfall and storm surge hazard models that are described in section 3.

Table 1. BoM best track data for Cyclone Marcia (2015) for 17/02/15 at 00 UTC – 20/02/15 at 18 UTC.

Date	Time (UTC)	Latitude	Longitude	Cp [hPa]	RMW [km]	Maximum Gust WS [ms^{-1}]	Category
17/02/2015	00:00	-14.40	155.50	1000	---	23.2	---
17/02/2015	06:00	-14.80	155.60	999	---	23.2	---
17/02/2015	12:00	-15.20	156.10	999	---	23.2	---
17/02/2015	18:00	-15.60	156.10	996	---	23.2	---
18/02/2015	00:00	-16.40	155.80	996	37	25.7	1
18/02/2015	06:00	-17.20	155.30	995	37	25.7	1
18/02/2015	12:00	-18.10	154.30	990	33	36	2
18/02/2015	18:00	-19.10	153.20	989	28	36	2
19/02/2015	00:00	-20.00	152.00	979	22	46.3	3
19/02/2015	06:00	-20.55	150.85	948	19	69.5	4
19/02/2015	08:32	-20.55	150.60	943	19	72	4
19/02/2015	12:00	-20.85	150.50	938	19	74.6	4
19/02/2015	18:00	-21.60	150.50	932	15	79.7	5
20/02/2015	00:00	-22.75	150.45	935	17	79.7	5
20/02/2015	03:00	-23.20	150.50	969	---	56.6	3
20/02/2015	06:00	-23.80	150.60	980	19	38.6	2
20/02/2015	12:00	-24.60	151.30	994	---	23.2	---
20/02/2015	18:00	-25.40	151.80	999	---	23.2	---

With the ensemble mean storm intensity parameters defined, a random distribution of the RMW, C_p, P_n and Holland B parameter values was generated to establish storm intensities for the entire ensemble event set (Figure 4). Taking a closer look at the randomly generated ensemble storm intensity parameters, the greatest variability is noted between the 60 hr and 78 hr forecast points, particularly in C_p and the Holland B parameter, which specifically help define the cyclone pressure fields. This variability will help create a diversity of storm intensities and impacts at landfall. Once the storm intensity parameters were assigned to the entire ensemble event set, the storm intensity parameters and position data were interpolated to a ten-minute time interval. This step was taken to simulate the hazards discussed in section 3 with finer temporal resolution than previous scenarios.

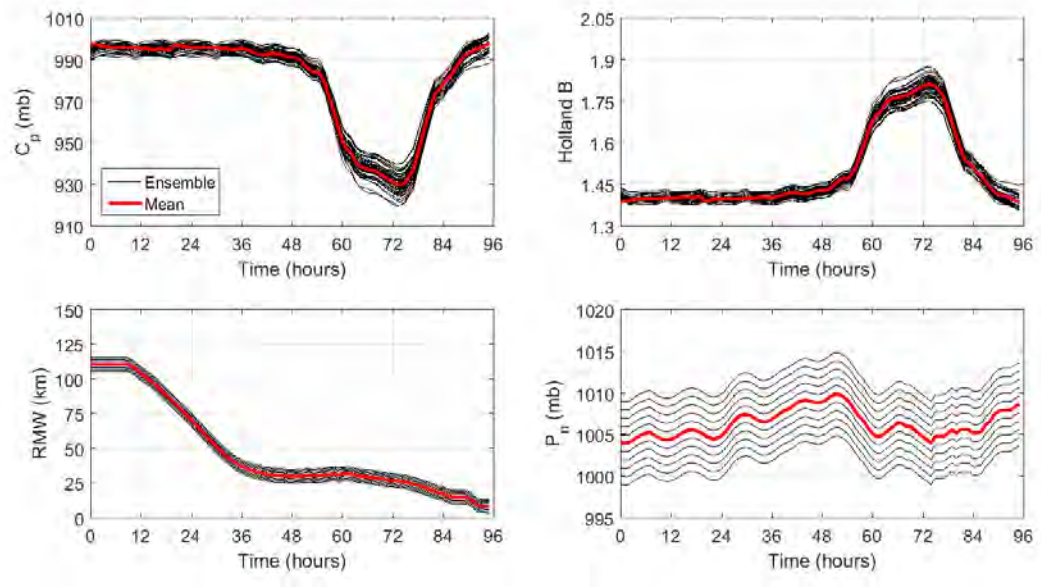

Figure 4. Modified 72 hr ECMWF ensemble and ensemble mean minimum central pressure (C_p), Holland B parameter, radius of maximum wind (RMW) and environmental pressure (P_n).

3 MULTI-HAZARD MODEL FRAMEWORK

Specific information on the surface terrain, topography, social demographic, building type, etc. was needed to properly simulate building damage and impacts on society in the study region. In Mason (2015), the National Exposure Information System (NEXIS) 2011 database was used to source aggregated statistics on the total number of dwellings (e.g. commercial, industrial, or residential), total number of occupants in residential dwellings, and building year (i.e. pre-1981 vs post-1981). These exposure statistics have been aggregated to different statistical areas (SAs) by Geoscience Australia. Mason (2015) leveraged coarser SA2 exposure statistics to represent the community level exposure that emergency management decisions would be based on. He also assigned a constant surface roughness length, z_0, to over land (z_0 = 0.02 m) and over water (z_0 = 0.002 m) regions and ignored the influence of topography and shielding. For this scenario, several improvements to the exposure dataset were made to include more realistically simulate damage and impact statistics at building level.

First, Geocoded – National Address File (G-NAF) data was sourced to assign a building classification (i.e. apartment, house, shop, factory, etc.) to a specific geocoded address (Figure 5). Not every point had a building classification associated with it in the G-NAF database, so synthetic values for building type, building year and total number of inhabitants were randomly assigned based on proportions that aggregated to match NEXIS 2011 SA1 statistics.

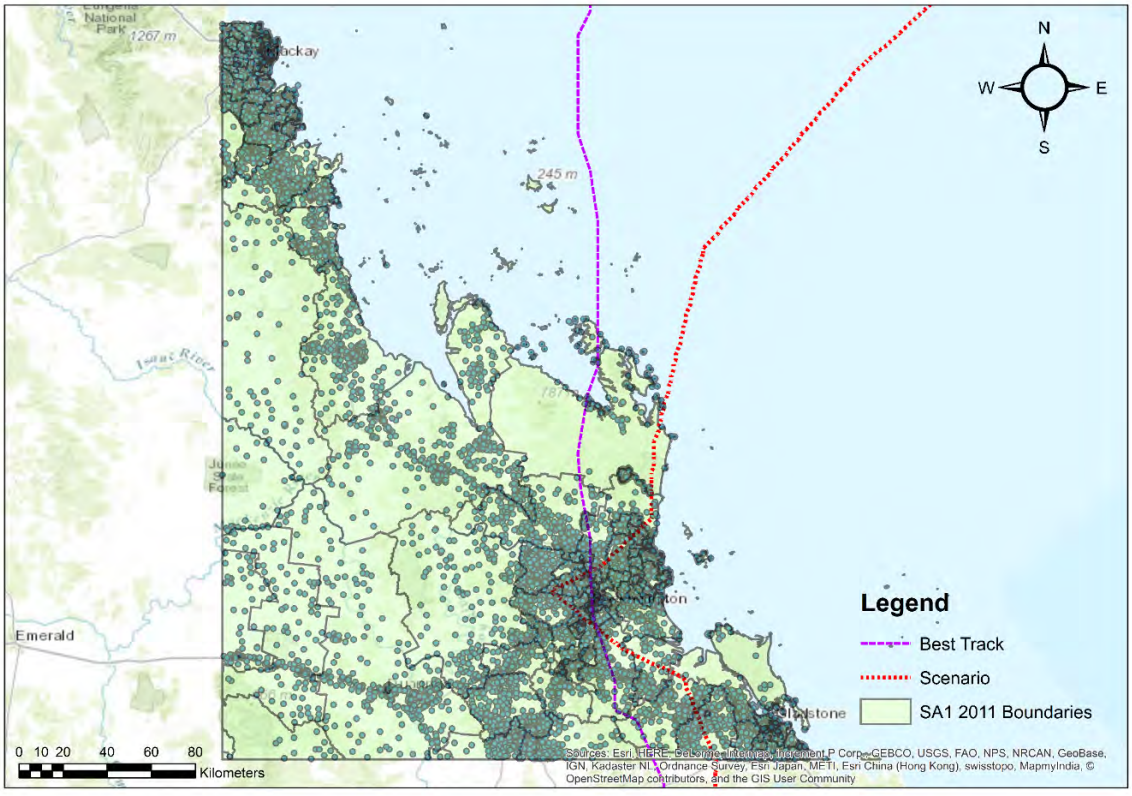

Figure 5. Same as Figure 2 but with synthetic G-NAF building locations displayed (filled circles).

Second, using the most recent 250 m horizontal resolution national Dynamic Land Cover Data (DLCD) provided by Geoscience Australia (2014) and z_0 tables from the peer reviewed literature (Wieringa 1992), individual z_0 values were assigned to each DLCD category (Table 2). For over water regions, a z_0 value of 0.002 m was still used. Single z_0 values represent an

effective value for each 5 km x 5 km grid point used to generate the regional wind fields for each ECMWF ensemble storm track. The authors acknowledge that future versions of the exposure dataset need to consider multiple changes in surface roughness upstream from the grid points to better represent the local effects of surface terrain on simulated regional wind fields.

Table 2. Surface roughness length values assigned to Geoscience Australia DLCD class names.

Class name	z_0 (m)
Extraction Sites	0.01
Inland Water Bodies	0.0005
Salt Lakes	0.0005
Irrigated Cropping	0.03
Irrigated Pasture	0.02
Irrigated Sugar	0.03
Rainfed Cropping	0.03
Rainfed Pasture	0.02
Rainfed Sugar	0.03
Wetlands	0.001
Tussock Grasses - Closed	0.05
Alpine Grasses - Open	0.01
Hummock Grasses - Open	0.01
Tussick Grasses - Open	0.01
Shrubs and Grasses - Sparse-Scattered	0.2
Shrubs - Closed	0.4
Shrubs - Open	0.2
Trees - Closed	0.8
Trees - Open	0.6
Trees - Scattered	0.6
Trees - Sparse	0.6
Urban Areas	1

Third, national wind multipliers from Geoscience Australia were sourced to adjust regional, open exposure maximum three-second gust wind speeds to site-relative, open exposure maximum three second gust wind speeds. The national wind multipliers account for local surface terrain, topography and shielding effects (Yang 2016) at each building using the approach outlined in AS/NZS 1170.2. Geoscience Australia provides them in tiles that contain eight netcdf files for each cardinal wind direction (starting from 0^o – 360^o at 45^o intervals) and specific multiplier (e.g. terrain, topography and shielding). Each netcdf file has a horizontal resolution of 50 m x 50 m. The tiles that were used to extract the netcdf files for the study region are displayed in Figure 6. Using the Data Management toolbox in ArcGIS, the netcdf files for each cardinal direction, specific multiplier and tile were merged into eight separate mosaic tiff files, so that for a given wind angle, a multiplier could be assigned to each building location to adjust regional wind speeds to site-relative wind speeds.

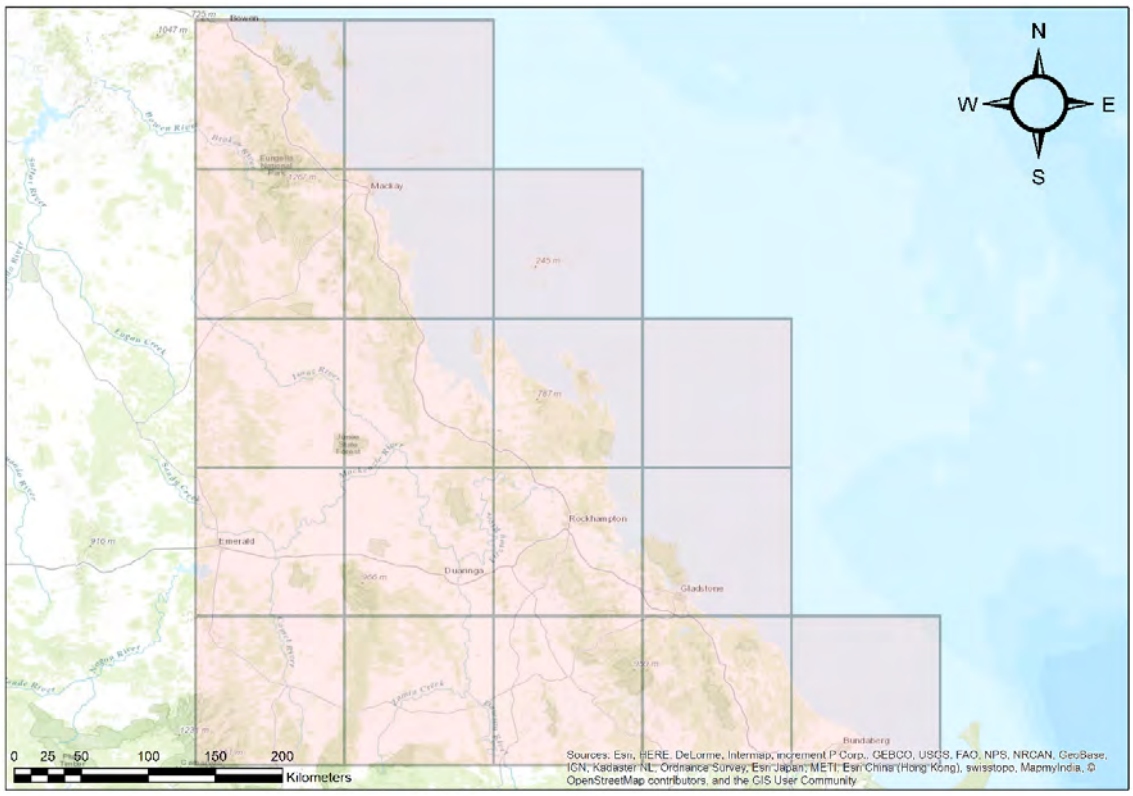

Figure 6. Geoscience Australia national wind multiplier tiles over the study region.

3.1 Hazard modelling

Tropical cyclones generate multiple hazards (i.e. wind, rainfall, and storm surge) that affect structures, critical infrastructure and society. It is important to model all hazards individually so both individual and combined hazard impacts can be quantified at landfall. To date, only the wind hazard has been considered in previous tropical cyclone scenarios (Mason 2015). This scenario improves upon the wind hazard model through the inclusion of a synoptic wind component, better treatment of surface roughness and topography (described in Section 2) and an increase in the horizontal grid resolution. Furthermore, capacity is added to the scenario risk model through the inclusion of rainfall and storm surge hazard models. The improvements are described in further detail throughout this section.

3.1.1 Wind field modelling

The wind hazard model used in previous reports (Mason 2015; Mason and Krupar 2015) has been updated to include a synoptic wind component using the approach outlined in Lin and Chavas (2012). The synoptic wind component is estimated by decelerating the translation speed by 55% and rotating the wind bearing 20^o clockwise (counter-clockwise) in the Southern (Northern) Hemisphere. Instantaneous earth-relative wind speed and direction are still calculated at an elevation of 10 m; however, the wind field horizontal and temporal resolution has been updated to 5 km x 5 km and ten-minute time steps respectively. Instantaneous wind fields simulated over water and land were adjusted for changes in underlying surface roughness using the 250 m horizontal resolution DLCD provided by Geoscience Australia (Table 2). Then, regional wind speeds were adjusted to open exposure terrain conditions (i.e. z_0 = 0.02 m) using a similarity model described in Simiu and Scanlan (1996) and a three-second time average using an empirical gust factor formula also described in Simiu and Scanlan (1996). An

example of one of the new regional maximum three-second gust wind fields adjusted to open exposure surface terrain conditions is shown in Figure 7. Once the regional wind fields have been adjusted to a common surface terrain exposure and time average, the three-second wind gusts at each 5 km x 5 km grid point were then interpolated to the synthetic exposure dataset grid points and multiplied by terrain, topography and shielding multipliers provided by Geoscience Australia to obtain the site-relative maximum three-second gust wind field (Figure 8).

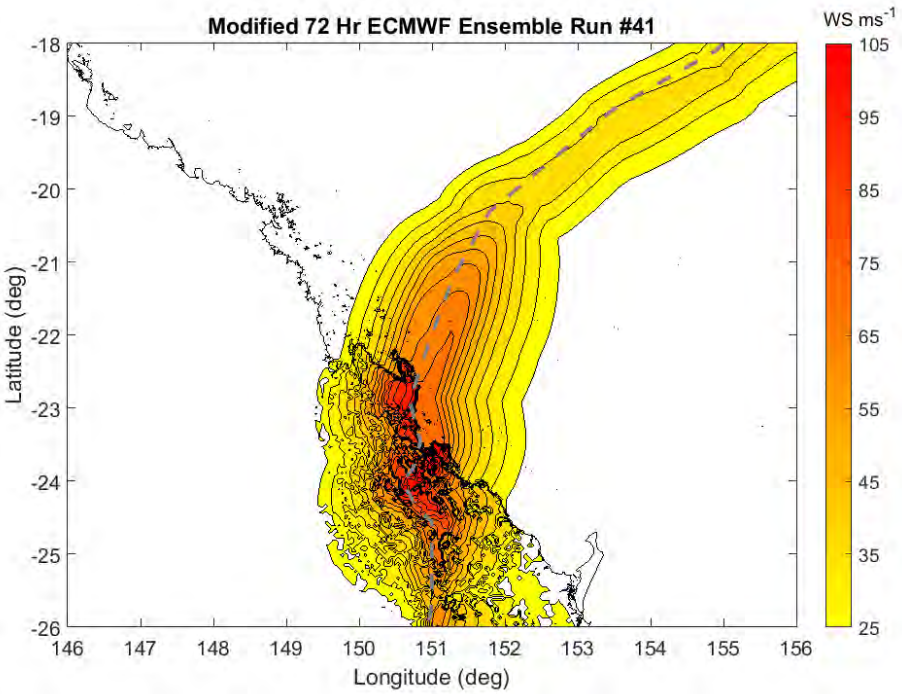

Figure 7. Modified 72 hr ECMWF ensemble run #41 regional maximum three-second gust wind field. The storm track is overlaid as a dashed grey line.

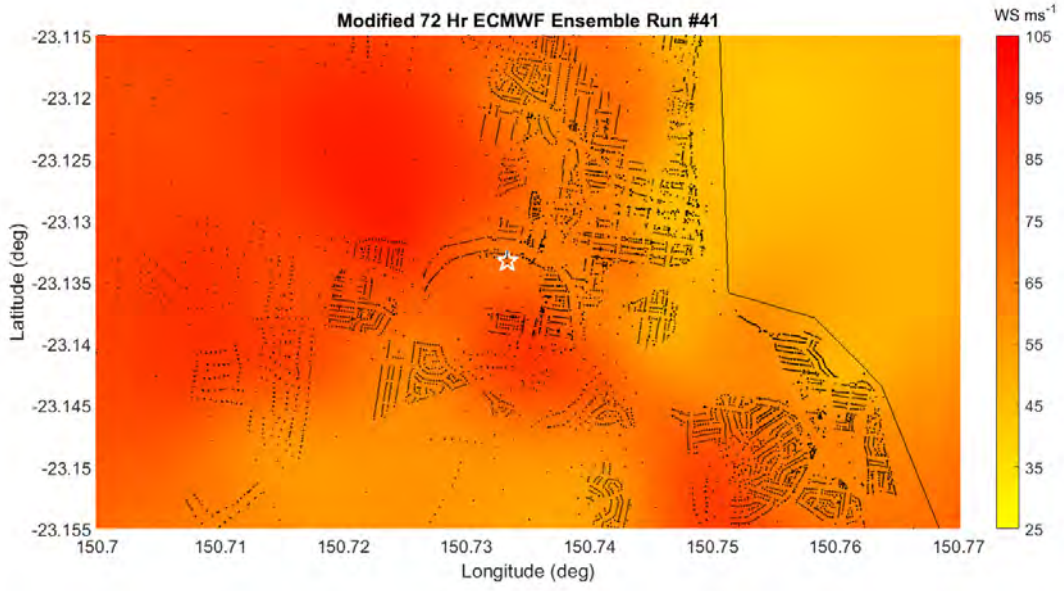

Figure 8. Modified 72 hr ECMWF ensemble run #41 site-relative maximum three-second gust wind field over Yeppoon.

3.1.2 Rainfall modelling

A refined rainfall climatology and persistence (R-CLIPER) model based on a satellite climatology of Tropical Rainfall Measuring Mission (TRMM) rainfall rates conducted by Lonfat et al. (2004) has been added to the multi-hazard modelling framework to estimate accumulated rainfall. Specific details on the TRMM R-CLIPER model algorithms and coefficients can be found in Tuleya et al. (2007). The TRMM R-CLIPER model requires an estimate of storm intensity (i.e. maximum wind speed in knots) and storm radius to approximate rainfall rates (in. day^{-1}) within 500 km of the storm centre (rainbands are not modelled in this version of the rainfall hazard model). The wind speed averaging time used to define the storm intensity is not specified in Tuleya et al. (2007), so a three-second time average is used. Also, the output rainfall rate is converted to mm $10\text{-}min^{-1}$ to match the temporal resolution of the wind field in the metric system. Coefficients for rainfall rates over land and water are provided for U.S. hurricanes, however, the over land coefficients still need to be calibrated for Australian surface terrain and topography conditions to adequately model Australian tropical cyclone rainfall. This calibration step was not taken in this scenario because a runoff model was not developed to model inland flooding and impacts associated with it. Future research will include development of a runoff model coupled with a fully calibrated rainfall hazard model to account for Australian surface terrain and topographic influences on tropical cyclone rainfall simulated at landfall and post-landfall.

3.1.3 Storm tide modelling

A proprietary license for Two-dimensional Unsteady FLOW Finite Volume (TUFLOW FV) was obtained from BMT WBM to model the storm tide along the Queensland. TUFLOW FV is a flexible mesh finite volume hydrodynamic numerical model that solves the non-linear shallow water equations to simulate hydrodynamic processes (e.g. storm tide, storm surge, etc.), sediment transport and water quality processes in different water bodies. For two-dimensional simulations of storm tide, the hydrodynamic model requires input pressure and wind fields, which are derived from the wind hazard model. Ocean tidal predictions are drawn from TPX08-atlas (Egbert and Erofeeva 2002) to establish boundary conditions for the flexible mesh. Waves can also be simulated using Simulating WAves Nearshore (SWAN), however, their impacts on structures were not examined for this scenario. Future scenarios should consider the effects of waves on structures and critical infrastructure at landfall.

Storm tide heights were estimated in the study region by first obtaining oceanic bathymetry data for the entire Coral Sea (Figure 9). Two data sources were required to inspect bathymetry values to the Coral Sea model mesh grid (Beaman 2010; Whiteway 2009). Once the bathymetry data had been sourced, a flexible finite volume mesh grid with unstructured triangular cells was created for the entire Coral Sea using Aquaveo's SMS 11.1 software package (Figure 10). Multiple boundaries were created to gradually decrease the horizontal resolution of the mesh vertices from approximately 30 km at the mesh boundary to 100 m (which was the smallest horizontal resolution between the two bathymetry datasets used in this scenario) near the coastline to adequately resolve the complex water levels along the coast. Once the model was created, ocean tidal data from 2015 was sourced from Queensland Government storm tide gauges in and around the study region to calibrate the Coral Sea model. During calibration, additional mesh modifications were required to match the observed and predicted storm tides. These additional modifications included embedding channels in the Great Barrier Reef to permit more water to flow through to the Queensland Coast, as well as, establishing material properties (i.e. surface roughness conditions) for the northern and southern boundaries of the Coral Sea model, the Great Barrier Reef and channels.

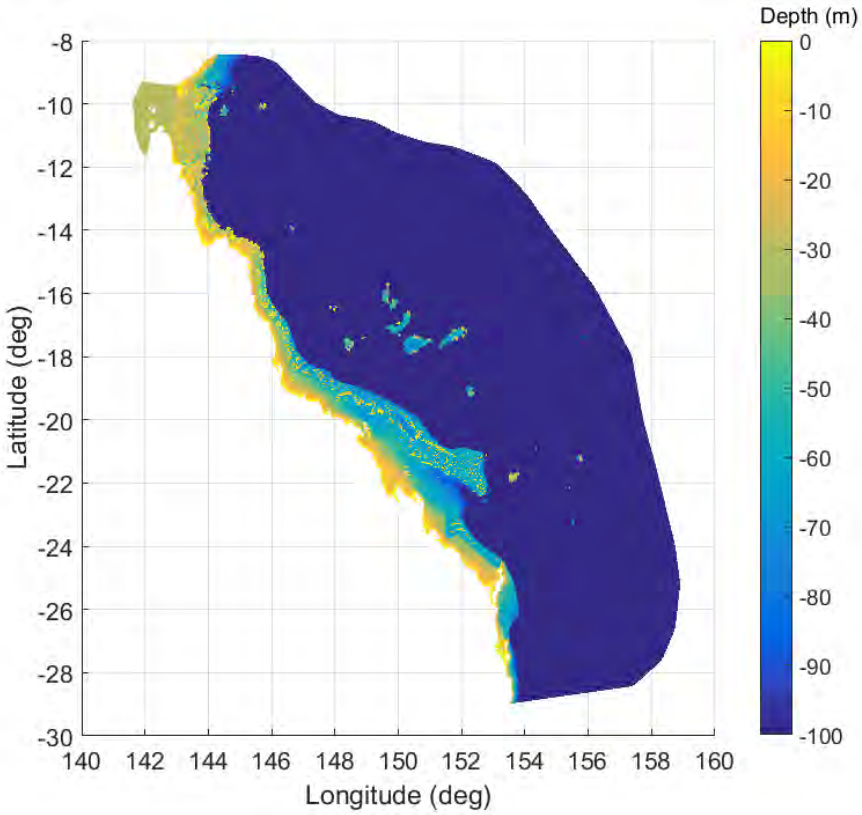

Figure 9. Bathymetry data for the Coral Sea storm tide hazard model.

Figure 10. Flexible finite volume triangular mesh used for storm tide modelling in the Coral Sea.

3.2 Vulnerability modelling

A preliminary assessment of publically available wind and flood vulnerability models that relate tropical cyclone hazards (wind, wind driven rain and storm tide) to building and infrastructure damage is presented in Mason and Parackal (2015). They highlight the relatively sparse availability of detailed (Australian) models and suggest that for disaster scenario analysis (wind and storm tide damage only) a modified version of the suite of building damage functions (curves) developed by Geoscience Australia be implemented as the basis for estimating building damage and subsequent population displacement. Justification for this recommendation is provided in that document and the reader is directed there for further clarification.

3.2.1 Wind vulnerability models

Figure 11 presents the aggregated and modified version of the Geoscience Australia wind vulnerability curves used for this scenario. This suite of curves has been used in previous tropical cyclone scenarios (Mason 2015; Mason and Krupar 2015) and includes curves for buildings in cyclonic (C) and non-cyclonic (N) wind regions, and for residential or commercial/industrial buildings. Additionally, different curves are used to differentiate between the expected impact on buildings constructed prior to (pre 1981) and following (post 1981) the introduction of stringent wind resistant design practice in Queensland (Walker 1995). The uncertainty in mean damage index across the study region was evaluated by using a random value between ± 5% of the calculated mean value determined using the vulnerability models displayed in Figure 11. For the town-specific uncertainty in mean damage index, a random sample of values from within pre-defined radii measured from the town centres (5 km for Byfield and 8 km for Rockhampton and Yeppoon) and equal to the total number of buildings in the radii was drawn from a Beta distribution about the mean damage index with the regional uncertainty included. For more specific details on the uncertainty models employed in this scenario, the readers are directed to Mason (2015). All implemented curves and uncertainty models should be considered as preliminary and subject to change in future work as results from the Bushfire and Natural Hazards CRC project "Improving the resilience of existing housing to severe wind events," become available for implementation.

Using the new synthetic exposure dataset described in Section 2 coupled with the wind vulnerability model (including the uncertainty models) just described, regional and town-specific mean damage indices are simulated at each individual building (i.e. residential, commercial and industrial) using the maximum site-relative gust wind speed (three-second time averaged wind speed at 10 m above ground level in open exposure) from each simulation. Then, following Smith and Henderson (2015), building damage states are computed (e.g. DS1, DS2 and DS3, which correspond to minor, moderate and severe damage). The number of buildings (both pre-1981 and post-1981) in each damage state is counted across the study region and within town-specific radii around Byfield, Rockhampton and Yeppoon. These three towns were selected for a more detailed analysis because they were identified as the hardest impact towns in the region during Cyclone Marcia.

It was also of interest to estimate the potential number of displaced persons so the requirements for alternate accommodation can be planned for. Displacement is defined here as the need for housing following an event, not the number of people requiring shelter during the event. The method utilised here for estimating displacement follows the HAZUS methodology (FEMA 2009) and is explicitly linked to residential building damage (see Mason 2015). Like the

damage state analysis, the number of people displaced from their pre-1981 and post-1981 homes are counted regionally and within town-specific radii.

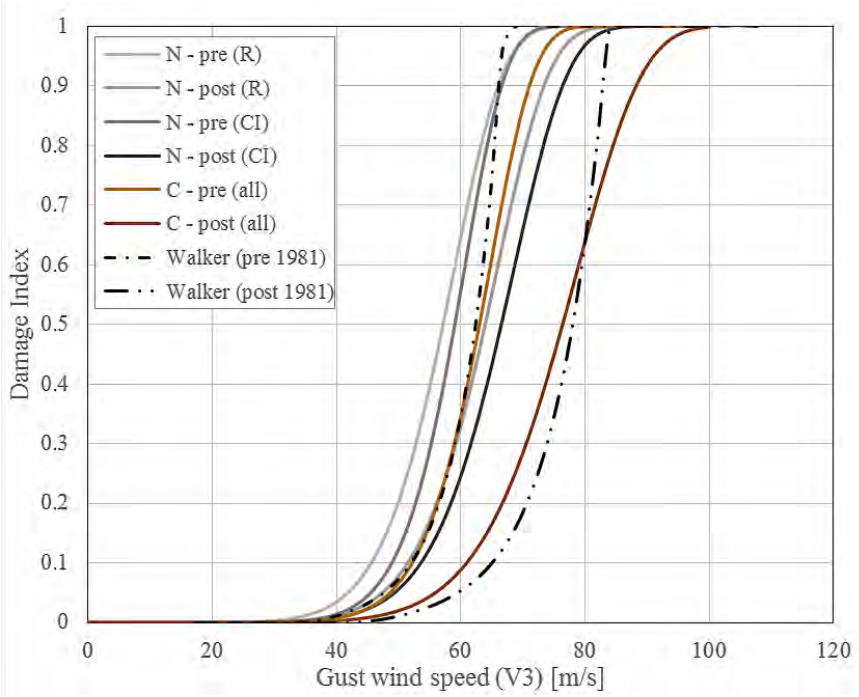

Figure 11. Vulnerability curves implemented in the current scenario analysis. Walker curves are shown for reference. N denotes non-cyclonic wind regions (Regions A and B in AS/NZS1170.2) with C indicating cyclonic (Region C). R indicates curves used for residential construction and CI for commercial and industrial buildings.

The estimation of wind-induced loss is calculated by multiplying the mean damage index at each synthetic building by the value of that building. Building values are drawn from a lognormal distribution of possible values with a total sum equal to the SA1 structural values provided in NEXIS 2011 for each building type (e.g. commercial, industrial and residential). Based on the Department of Infrastructure and Regional Development residential building prices, residential building values did not change all that much from 2011 – 2015. Given this information, NEXIS 2011 residential, commercial and industrial building values were applied to the synthetic building exposure dataset. It is assumed that building values and estimated mean damage indices are independent and are randomly matched like Mason (2015). Regional losses are then estimated by aggregating loss from each statistical pre-1981 and post-1981 building across the study region depending on the degree of damage and within the town-specific radii.

3.2.2 Flood vulnerability models

With the addition of the storm tide hazard model, building damage and impacts to their inhabitants were desired. Mason and Parackal (2015) provide a comprehensive overview of flood vulnerability modelling and suggest that the total loss ratio (which include both building and contents damage) versus inundation depth flood vulnerability curves developed in Mason et al. (2012) be employed in flood disaster scenario simulations. These curves embody the Geoscience Australia flood vulnerability curves but differ in that they are adjusted for Queensland building construction and are based on claims data from the 2011 Queensland floods. The Simplified Building Type (SBT) total loss ratio versus inundation curves developed in Mason et al. (2012) are shown in Figure 12. The curves assume slow rising floods, which mostly results in contents/lining damage and not major structural damage. The flow velocity

must be accounted for to adequately determine structural impacts. Given that a bath-tub approach is used to simulate storm tide heights at the coastal interface of the study region and inland flow velocities are not simulated, structural losses are not considered in this scenario.

Using only the inundation depth curves in Figure 12 will result in an underestimation of storm tide-related damage, however, future work will explore how to model inland flow velocities so structural impacts and losses can be examined at building level in future scenarios. The uncertainty in total loss ratio across the study region was evaluated by using a random value between ± 3% of the calculated mean value determined using the vulnerability models displayed in Figure 12. For the building level total loss ratios, a random sample was drawn from a Beta distribution about the mean total loss ratio with the regional uncertainty included. Alpha and beta parameters for the random sampling were defined using the approach outlined in (Egorova et al. 2008). For more specific details on the flood vulnerability models employed, the readers are directed to Mason et al. (2012).

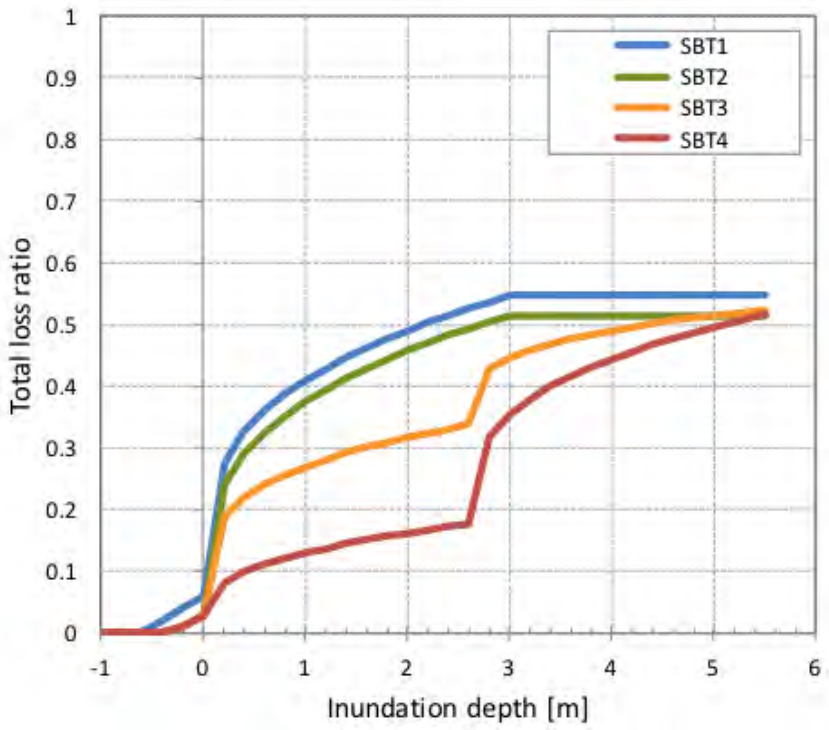

Figure 12. Total loss ratio versus inundation depth mean curves from Mason et al. (2012).

To simulate impacts on society (i.e. displaced inhabitants), the methodology in HAZUS-MH flood loss model (FEMA 2013) was adopted. The overarching factor controlling the method is physical access into the region where the statistical buildings are impacted. As such, this is a function of the ability to reach the building either on foot or by vehicle. For this scenario, it was assumed that if the storm tide depth reached 0.2 m that residents were unable to return to their property. It should be noted that residents are never encouraged to walk through storm tide water during or after tropical cyclone events transpire. Given these storm tide depth assumptions, the HAZUS-MH flood model method for estimating displaced inhabitants was employed:

$$D_{IN} = \sum_{j=1}^{n} POP_{IN} \quad (1)$$

where D_{IN} is the total number of people displaced from their home because the flood depth exceeds the assumed 0.5 m depth preventing return to a property, n is the total number of buildings in a census block or pre-defined region and POP_{IN} is the total number of people located within a census block or pre-defined region.

For this scenario, the maximum storm tide heights for each modified 72 hr ECMWF ensemble storm track simulation just offshore from the study region were used to simulate building and contents damage, as well as, population displacement in and around Yeppoon. Yeppoon was the focal point of this portion of the analysis because Byfield and Rockhampton are located far enough inland that neither town would experience storm tide impacts. These towns would suffer from inland flooding due to heavy rainfall in the nearby catchment (as evidenced by the recent impact of Cyclone Debbie in 2017), but this analysis has not been carried out for this scenario due to time constraints. Simulated fatalities have also been neglected in this scenario given that the age of residents within their respective dwellings is not quantified in NEXIS 2011 or G-NAF, which makes it difficult to generate realistic simulations of potential fatalities in this tropical cyclone disaster impact scenario. If age and wealth information can be sourced, future work will incorporate potential fatalities due to storm tide.

4 SCENARIO RESULTS

4.1 Simulated wind fields

To examine the distribution of maximum site-relative gust wind speeds for each simulation across the study region and in Byfield, Rockhampton and Yeppoon, the maximum regional gust wind field for each simulation was interpolated to the location of the synthetic exposure dataset described in Section 2. Local modifications for surface terrain, topography and shielding were made using the Geoscience Australia wind multipliers to obtain site-relative gust wind speeds. Point density maximum site-relative gust wind speed maps were generated for each simulation and then the distribution of the gusts across the entire ensemble set was examined in closer detail across study region (Figure 13).

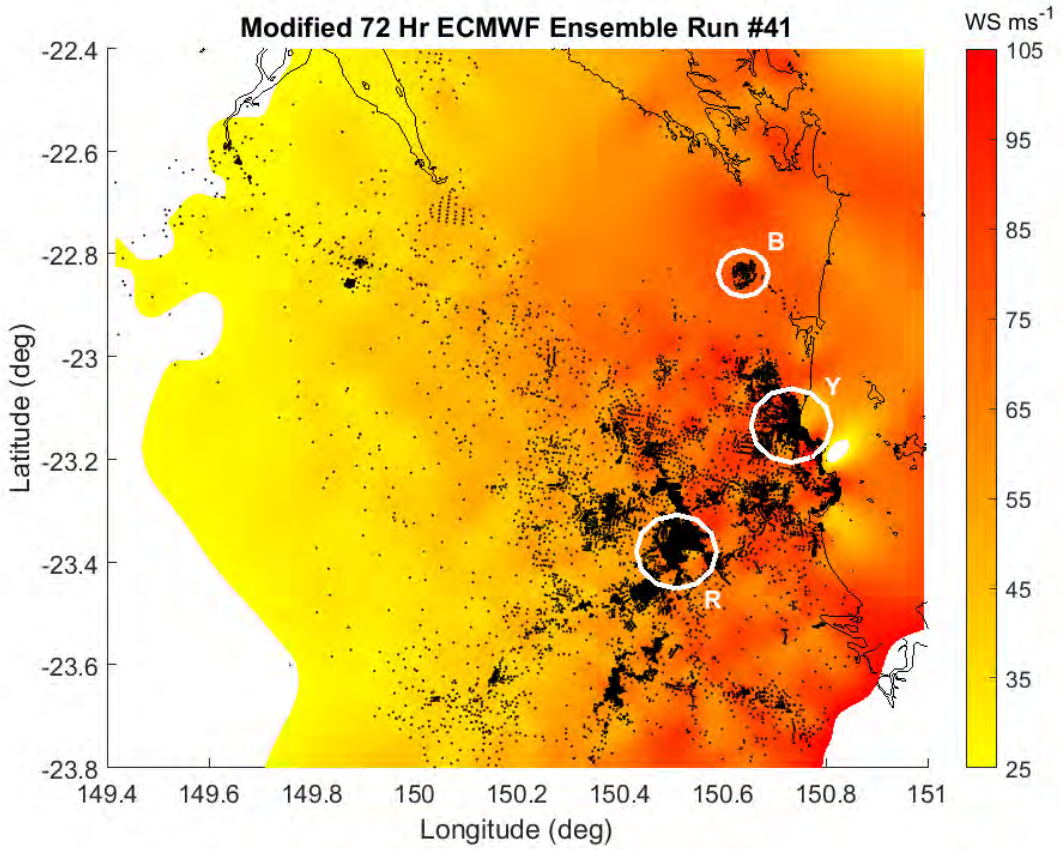

Figure 13. The site-relative gust wind speed footprint derived from modified 72 hr ECMWF ensemble run #41. Wind speeds are three-second averaged gusts at 10 m over open terrain and account for surface terrain, topographic and shielding effects. Byfield (B), Rockhampton (R) and Yeppoon (Y) are encircled with a 5 km, 8 km and 8 km radius measured from each town centre respectively.

The maximum gust wind speed across the entire ensemble event set was simulated to be 122.49 ms^{-1} (440.96 kmh^{-1}) and occurred during ECMWF ensemble run #47 on the northeast edge of Rockhampton. The remainder of the site-relative gust wind speed was well above 75 ms^{-1} in Byfield, Rockhampton and Yeppoon. Empirical cumulative distributions functions (ECDFs) of the maximum site-relative gust wind speed for Byfield, Rockhampton and Yeppoon were created to examine the distribution of the gust wind speeds for the entire ensemble event set in and around each town (Figure 14).

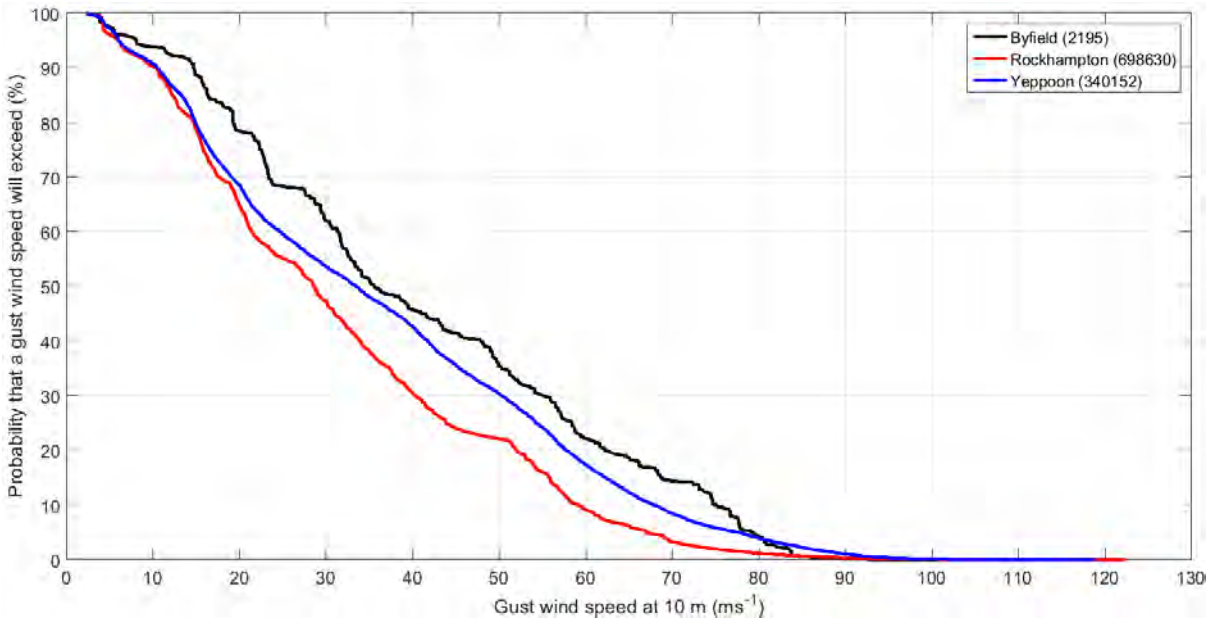

Figure 14. Empirical cumulative distribution functions (ECDFs) for site-relative maximum three-second gust wind speeds observed within 5 km of Byfield and 8 km of Rockhampton and Yeppoon. The total number of gust wind speeds from all fifty simulations in each ECDF is displayed in the legend.

These curves illustrate what the probability of exceedance of a gust wind speed magnitude would be considering the entire event set (e.g. all fifty simulations). For this scenario, the maximum gust wind speeds overland exhibit a large range of magnitudes in and around each town. The greatest range of gust wind speeds is observed near Rockhampton (120.17 ms^{-1}), where 90% of the gust speeds are likely to be less than or equal to approximately 59 ms^{-1}. For Yeppoon and Byfield, there was a 10% probability of exceeding gust wind speeds at or above approximately 68 ms^{-1} and 75 ms^{-1} respectively. Depending on the risk appetite of the end user, an ECDF can be used in emergency decision making to evaluate the probability of a certain range of gusts wind speeds that might be experienced for a given ensemble forecast within and around select towns. These gusts wind speeds are now used to simulate damage to buildings and impacts on their inhabitants.

4.2 Wind-induced building damage

The maximum site-relative gust wind speed at each synthetic building from each simulation is used as input into the wind vulnerability model described in sub-section 3.2.1. to compute damage indices. The variability of the damage indices has been evaluated using the 50^{th}, 75^{th} and 90^{th} percentiles. Damage to residential, commercial and industrial buildings is discussed in this section (when applicable), with residential damage being of most importance to determining whether the structures are habitable and uninhabitable.

Figure 15 shows the spatial distribution of the 50^{th}, 75^{th} and 90^{th} percentile damage indices (with uncertainty included) for residential, commercial and industrial buildings (both pre-1981 and post-1981) across the study region. The damage index scale ranges from zero indicating no damage to one indicating repair/replacement costs equating to the value of the structure. Taking a closer look at the maps generated in Figure 15, some clear patterns and trends can be noted across all building types as the percentile range increases. First, an increase in the spatial coverage of damage is observed with increasing percentile range, with very low damage indices noted for the 50^{th} percentile (below 0.1) and much higher indices (> 0.5) at the 90^{th} percentile.

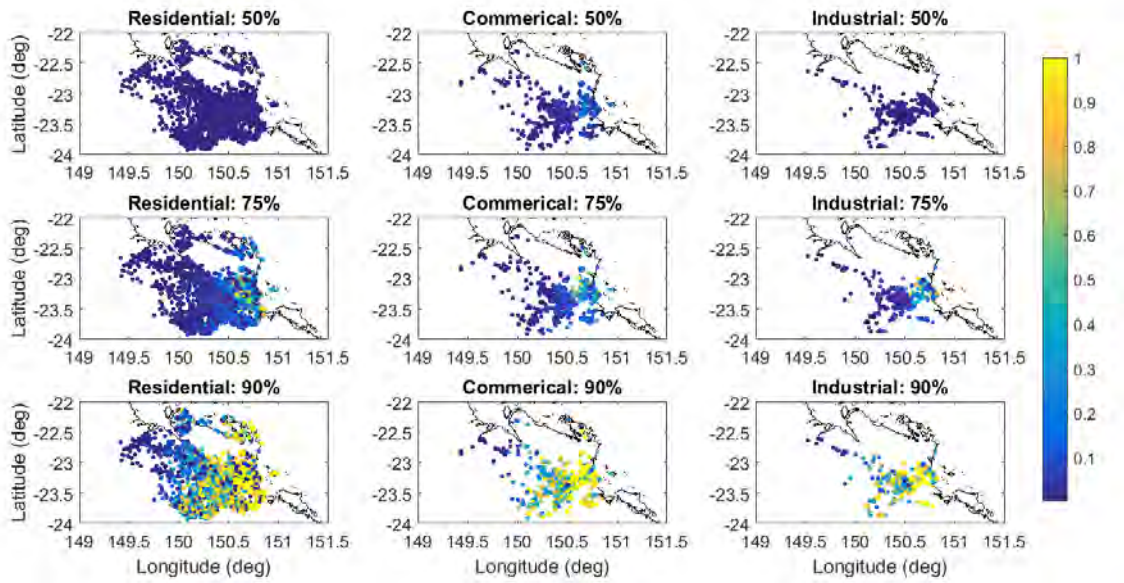

Figure 15. The 50th, 75th and 90th percentile damage indices for pre-1981 and post-1981 residential, commercial and industrial buildings combined across the study region.

This trend is not surprising given that more extreme gust wind speeds will be included at higher percentiles for the entire ensemble event set. Another interesting pattern is noted in the 75th percentile, where higher damage indices above 0.5 are observed along the eastern third of the study region for residential structures. For commercial and industrial buildings, the higher damage indices are located mostly between Rockhampton and Yeppoon, with some higher commercial damage also noted in Byfield. There were no industrial buildings in Byfield to examine in this exposure dataset.

To get a better impression of the distribution of damage indices for residential buildings in Byfield, Rockhampton and Yeppoon for each percentile, ECDF curves were generated for each building era (e.g. pre-1981 and post-1981) and are shown in Figure 16. The first thing to note is that the sample size between the three cities is significantly different (see legends of each plot for sample size values) for both pre-1981 and post-1981 building construction. However, the sample size is large enough for each town to examine the distribution of the damage indices reliably. It is evident that pre-1981 residential buildings in each town have a higher probability of moderate to high damage indices (i.e. 0.5 and above) than post-1981 residential buildings. This observation was expected given that pre-1981 residential buildings have been shown to be prone to higher damage at lower gust wind speeds than post-1981 building construction practice. Rockhampton appears to have a lower chance of reaching higher damage indices in this scenario compared to Byfield and Yeppoon and this is largely because it is farther inland and more removed from higher gust wind speeds generated in the ensemble event set. Byfield is the farthest north town and has the highest chance of experiencing moderate to severe damage compared to Rockhampton and Yeppoon.

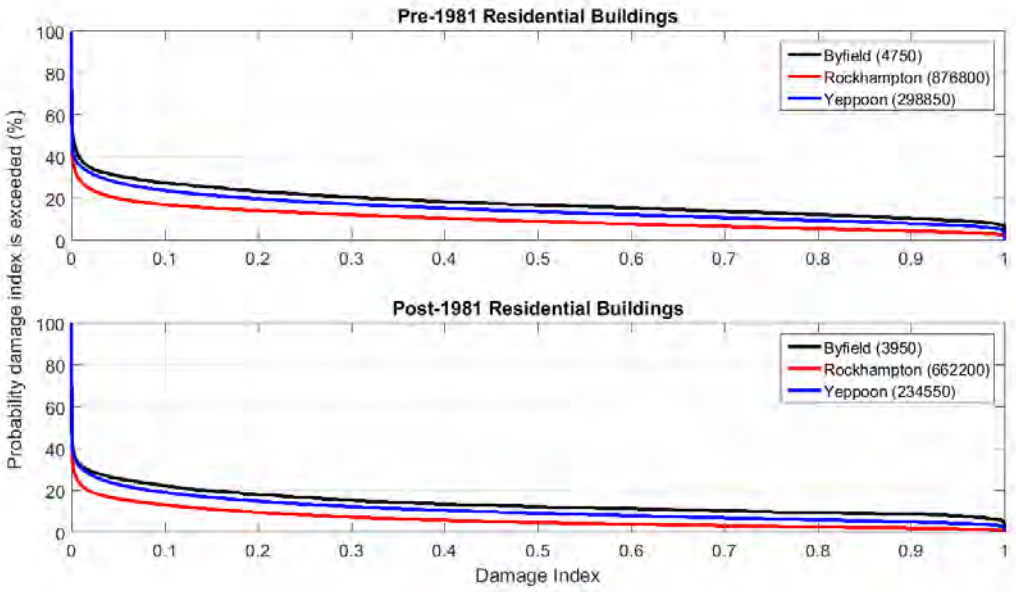

Figure 16. Empirical cumulative distribution functions (ECDFs) of mean damage index for pre-1981 and post-1981 residential buildings in Byfield, Rockhampton and Yeppoon.

While damage index distributions show damage relativities across the synthetic building exposure dataset, the actual level of impact is perhaps more clearly depicted by the number of buildings within a DS, or damage index range. As outlined in sub-section 3.2.1, three DSs are defined here, DS1 (minor), DS2 (moderate) and DS3 (major). Moderate and major damage states are of most importance to the scenario as buildings within these states present those that will require some level of repair/reconstruction that will require the occupants to seek alternate accommodation. While damage will be sustained by some buildings classified as DS1, repairs are not expected to render the building uninhabitable. Damage presented in this manner is meant for emergency/reconstruction/resilience planning.

Figure 17 presents maps of the damage state that each building and building type is classified as for the 50th, 75th and 90th percentile damage states for the entire ensemble event set. Most of if not all the residential, commercial and industrial buildings experience DS1 level damage at the 50th percentile. A noticeable increase in the degree of damage is noted at the 75th percentile across all the building types in response to the inclusion of higher gusts wind speeds. For example, a decrease of 20,895 residential homes in DS1 was observed between the 50th and 75th percentiles, while an increase of 17,196 and 3,699 houses was noted for DS2 and DS3 respectively. At the 90th percentile, a significant number of residential, commercial and industrial buildings experience severe damage (e.g. DS3). Roughly 43%, 45% and 46% of the total number of residential (62,762), commercial (3,619) and industrial (2,157) buildings have been classified as experiencing severe damage. These DS maps can be used in emergency management/disaster recovery planning risk assessments to evaluate the potential degree of damage buildings within a council may experience. Depending on the risk appetite of the end user, certain resources can be pre-allocated before an event or after landfall.

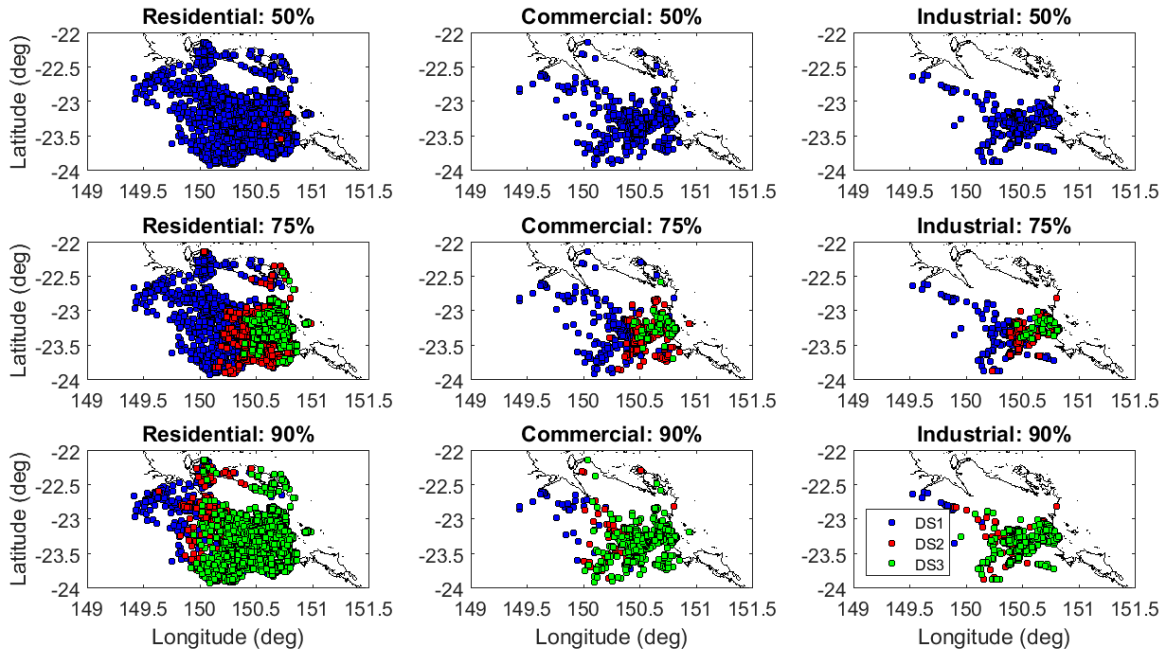

Figure 17. Damage state (DS) values experienced by residential, commercial and industrial buildings for the 50th, 75th and 90th percentile maximum site-relative gust wind speed footprints. The legend applies to all panels.

Counts of the total number of synthetic residential buildings in each damage state and percentile range around Byfield, Rockhampton and Yeppoon for pre-1981 and post-1981 building construction eras are displayed in Table 3. As was noted in Figure 17, the total number of DS1 homes (both pre-1981 and post-1981) decreases as the percentile range increases. Conversely, the total number of pre-1981 and post-1981 homes in DS3 increases with increasing percentile range. For DS2 homes, the total number of homes increased from the 50th to 75th percentile and then decreased from the 75th to 90th percentile for Byfield and Yeppoon, while an increase through the percentile range was noted over Rockhampton. This irregularity in the DS2 trends between the three towns is believed to be associated with the proximity of the towns to the storm strike location (i.e. landfall location), as well as, storm intensity and inland trajectory of each simulated storm. Depending on these three variables, more irregularities in the DS2 trends could be observed since Byfield and Yeppoon are closer to the landfall point of each simulated storm. General inland decay will also help create a more stabilized overall DS2 trend for a town like Rockhamtpon, which is positioned much farther inland. These sensitivities will be explored in future work.

Table 3. Damage state (DS) counts for Byfield, Rockhampton and Yeppoon for the 50th, 75th and 90th percentile maximum site-relative gust wind speed footprints. The residential DS values are broken down building construction era.

City name - percentile	DS1 (R_pre)	DS1 (R_post)	DS2 (R_pre)	DS2 (R_post)	DS3 (R_pre)	DS3 (R_post)
Byfield – 50th percentile	150	24	0	0	0	0
Byfield – 75th percentile	39	4	100	17	11	3
Byfield – 90th percentile	34	2	1	1	115	21
----------	----------	----------	----------	----------	----------	----------
Rockhampton – 50th percentile	15709	15071	0	0	0	0
Rockhampton – 75th percentile	11769	11612	3721	3273	219	186
Rockhampton – 90th percentile	5572	5336	4251	4495	5886	5240
----------	----------	----------	----------	----------	----------	----------
Yeppoon – 50th percentile	6886	3781	1	0	0	0
Yeppoon – 75th percentile	3126	1654	2657	1495	1104	632
Yeppoon – 90th percentile	1937	1042	1399	735	3551	2004

4.3 Wind-induced population displacement

Using the population displacement method described in Mason (2015) for residential construction, the living condition of each home in the study region was examined. Specific population displacement figures were withheld because representative information regarding the number of occupants living in each residence could not be determined for the G-NAF dataset. Figure 18 shows which homes were inhabitable or uninhabitable for the 50th, 75th and 90th percentile maximum site-relative gust wind speed footprints for both residential building construction eras. The total number of uninhabitable homes increases with increasing percentile range (e.g. increasing gust wind speed magnitude). All residential homes were habitable up to the 50th percentile, while roughly 6% and 43% of the total number of homes were uninhabitable for the 75th and 90th percentiles respectively. These maps can be used in emergency management/disaster recovery planning risk assessments to evaluate the potential number of people that may be displaced from their home or need shelter within a council. The shelter requirement is not addressed with this risk assessment and methodology, however, with more demographic information on the wealth of a region, emergency services managers can make more informed decisions on shelter requirements using the provided maps.

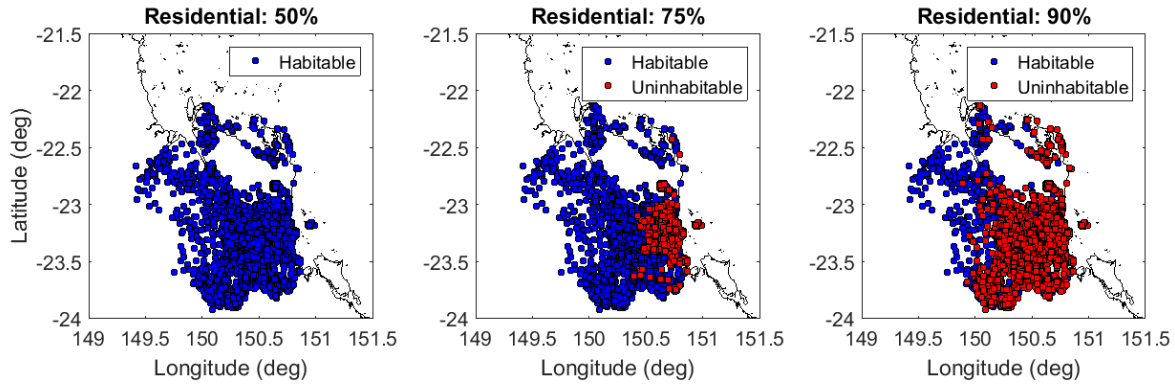

Figure 18. Inhabitable and uninhabitable residential buildings for the 50th, 75th and 90th percentile maximum site-relative gust wind speed footprints.

The total number of inhabitable and uninhabitable homes in Byfield, Rockhampton and Yeppoon was computed for each building era and percentile range, and the counts are displayed in Table 4. As the percentile range increases within each town, the total number of pre-1981 and post-1981 inhabitable homes decreases, while the total number of uninhabitable pre-1981 and post-1981 homes increases. Also, due to poor building practice in the pre-1981 building construction era, more pre-1981 homes are uninhabitable than homes built in the post-1981 building construction era.

Table 4. Total number of inhabitable and uninhabitable pre-1981 and post-1981 residential buildings for the 50th, 75th and 90th percentile maximum site-relative gust wind speed footprints in Byfield, Rockhampton and Yeppoon.

City name - percentile	Number of inhabitable buildings (pre – 1981)	Number of inhabitable buildings (post – 1981)	Number of uninhabitable buildings (pre – 1981)	Number of uninhabitable buildings (post – 1981)
Byfield – 50th percentile	150	24	0	0
Byfield – 75th percentile	139	21	11	3
Byfield – 90th percentile	35	3	115	21
----------	----------	----------	----------	----------
Rockhampton – 50th percentile	15709	15071	0	0
Rockhampton – 75th percentile	15490	14885	219	186
Rockhampton – 90th percentile	9823	9831	5886	5240
----------	----------	----------	----------	----------
Yeppoon – 50th percentile	6887	3781	0	0
Yeppoon – 75th percentile	5783	3149	1104	632
Yeppoon – 90th percentile	3336	1777	3551	2004

4.4 Simulated storm tide

Maximum storm tide heights from progressive ten-minute TUFLOW FV hydrodynamic simulations driven by each modified ECMWF ensemble storm track have been calculated between 00:00 AEST on 20 February 2015 and 00:00 AEST on 21 February 2015, during which time the peak astronomical tide was observed (2.98 m at 10:00 am AEST on 20 February 2015). These maximum simulated storm tide heights have been extracted from a location just offshore from Yeppoon and range from 1.23 m – 5.83 m for the entire ensemble set. The range of maximum simulated storm tide heights is so large because not all the ensemble simulations struck the Queensland Coast and/or study region in the same location, resulting in large variations in the wind-driven storm tide heights. The maximum simulated storm tide height (5.83 m) was observed during ensemble run #41 at 09:55 am AEST on 20 February 2015, which was five minutes before the observed peak astronomical tide (Figure 19). The maximum simulated storm tide height corresponds to a maximum simulated storm surge height of 2.85 m.

To examine residential housing and contents damage, as well as, the potential displacement of residents due to inaccessibility caused by the storm tide, the 50th and 75th percentile maximum simulated storm tide heights were used along with the maximum simulated storm tide height for the entire ensemble set. These storm tide heights were selected to allow end users (i.e. emergency services managers) to evaluate the potential storm tide risk across the synthetic exposure dataset based on their risk appetite.

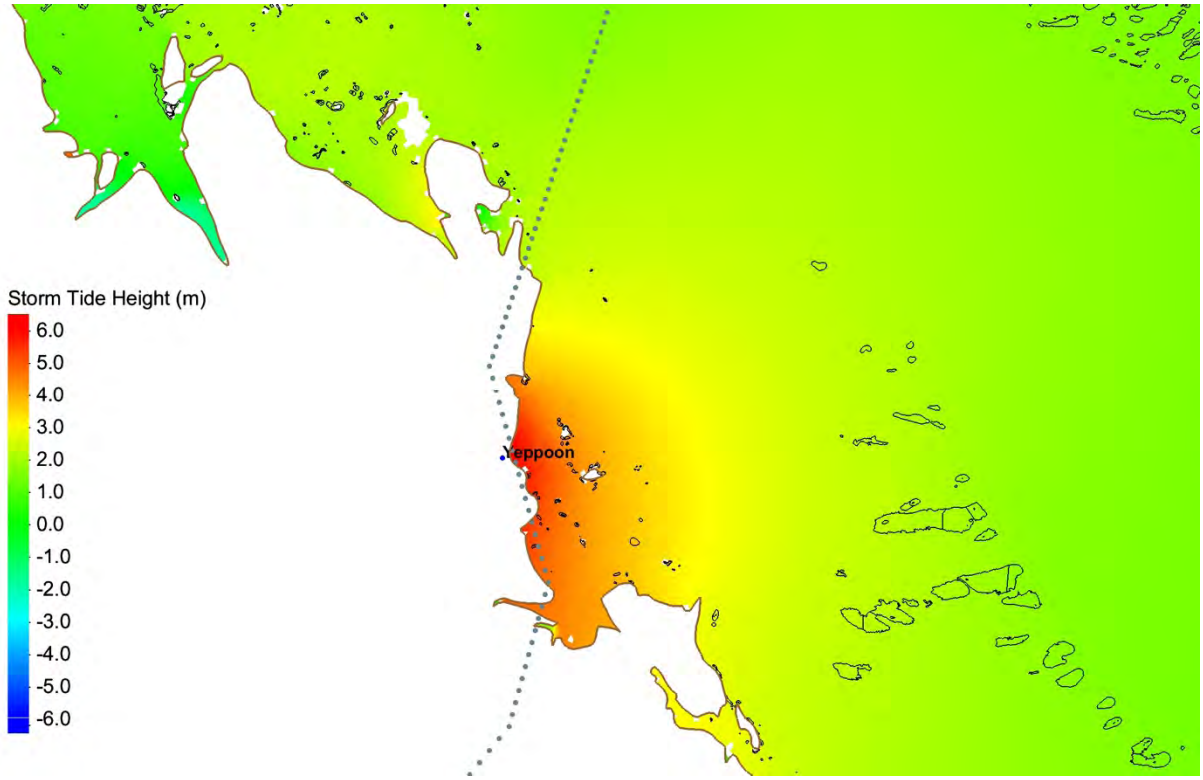

Figure 19. Modified 72 hr ECMWF ensemble run #41 storm tide simulation at 9:50 am AEST on 20 February 2015.

4.5 Storm tide-induced total loss ratios

A more localized region of synthetic houses (excluding apartment residences) was extracted from the larger synthetic exposure dataset to examine the distribution of simulated residential building and contents damage caused by the storm tide across the study region (Figure 20). Commercial and industrial buildings were not considered in this scenario, but impacts on these building types will be explored in future work. Since there was a lack of detailed information on the houses (i.e. one versus two-storey, floor height, etc.), the SBT categories developed by Mason (2012) were randomly assigned to the local synthetic residential building dataset. Furthermore, floor heights between 0.2 m and 0.5 m were also randomly assigned to each synthetic residential building. Using a bath-tub mapping approach, storm tide heights were simulated for each ensemble run and advected inland over the localized exposure dataset. Using high-resolution (i.e. 25 m horizontal resolution) topography data from the Queensland Government Queensland Spatial (QSpatial) Catalogue (DNRM 2005), the difference between the topography (plus the building floor height) and maximum storm tide heights is computed at the location of each synthetic building to determine the inundation depth (not shown). The inundation depth is then used as an input into the flood vulnerability model to simulate total loss ratios (building/contents damage) for each synthetic house according to its SBT categorical assignment.

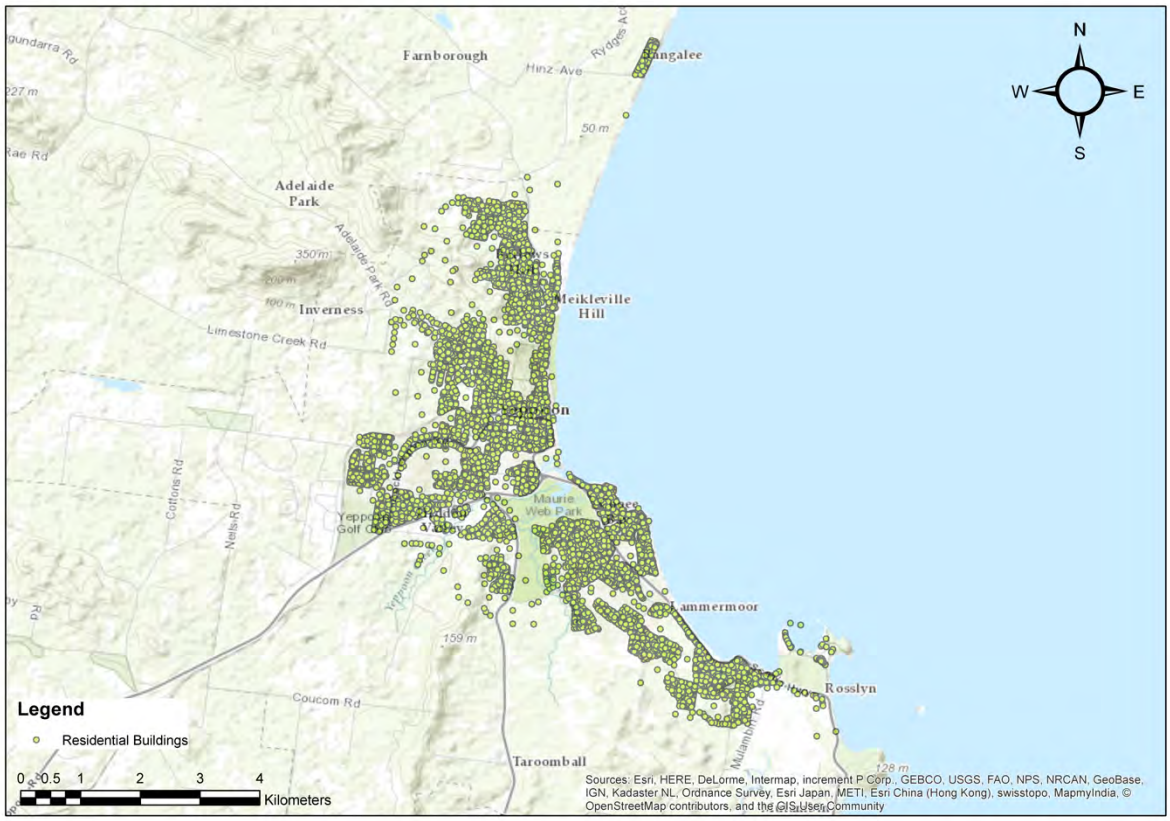

Figure 20. Synthetic houses extracted from the larger synthetic exposure dataset.

The 50th and 75th percentile maximum simulated storm tide heights for the entire ensemble event set are 2.75 m and 3.12 m respectively. For reference, the 90th percentile maximum simulated storm tide height is 4.18 m. The maximum simulated storm tide height of 5.83 m produced during ensemble run #41 is 1.65 m above the 90th percentile maximum storm tide height and is an extreme event with low probability of occurrence. Total loss ratios (including uncertainty) for each synthetic house are shown in Figure 21 for the 50th and 75th percentile maximum simulated storm tide heights, as well as, the maximum simulated storm tide height for the entire ensemble set. In general, as the storm tide height increases from 2.75 m to 3.12 m, the areas experiencing combined building and contents damage do not change. The primary damage areas are Bangalee, South Yeppoon (near the Yeppoon Inlet) and north of Capricorn Coast National Park. When the maximum simulated storm tide height observed across the entire ensemble set is used as an input in the flood vulnerability model, several more regions of potential building and contents damage arise. For example, several homes across South Yeppoon and Lammermoor experience high total loss ratios (>= 0.4). Moreover, the total loss ratio increases in magnitude over all the previously identified regions towards the high end of the scale, indicating that severe building and contents losses could potentially be experienced at or above this storm tide height.

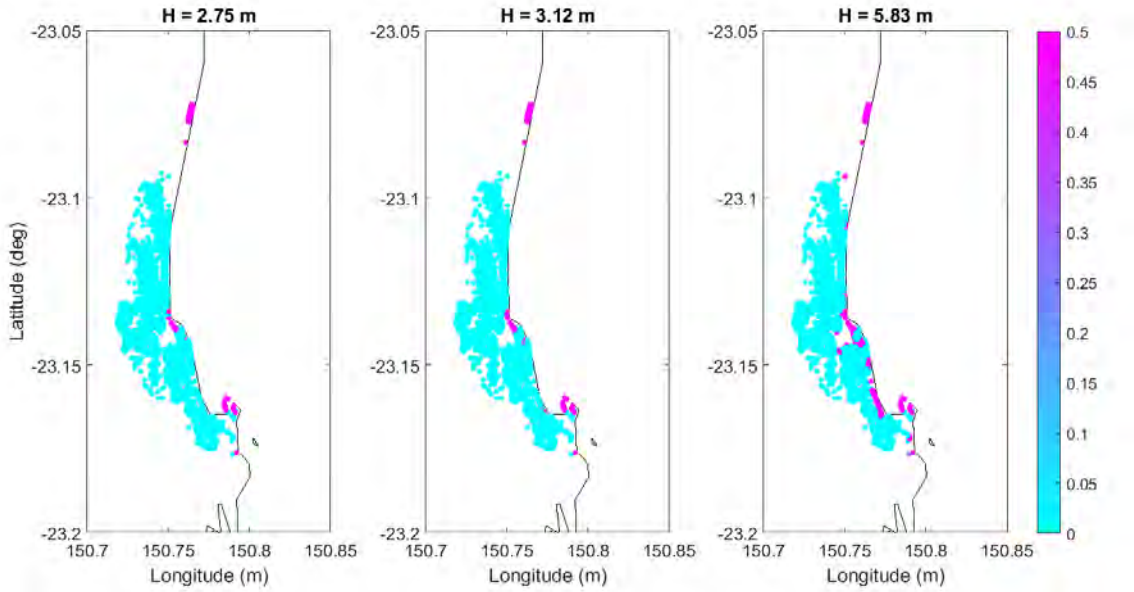

Figure 21. Total loss ratios for the 50th and 75th percentile maximum simulated storm tide footprint for each synthetic house. The maximum simulated storm tide height footprint for the entire ensemble event set is also displayed.

4.6 Storm tide-induced population displacement

Assuming everyone evacuated from their homes before each simulated storm arrived, the population displacement is determined based on the inundation area. Individuals or households will be displaced from their homes if they cannot physically re-enter their property due to flood depths. Unlike the wind risk assessment, the storm tide risk assessment does not consider structural damage as a key indicator for individual or household displacement. However, depending on the duration of time that a structure is immersed in a certain depth of water and the time that large waves impacted the structure, residents may or may not be displaced due to structural damage experienced. These variables are not considered in this scenario, but will be explored in future work.

Based on the criteria established in sub-section 3.2.2, residences were considered accessible or inaccessible for the 50th and 75th percentile maximum simulated storm tide heights, as well as, the maximum simulated storm tide height for the entire ensemble event set. The accessible and inaccessible houses are displayed in (Figure 22). The total number of accessible and inaccessible homes for each maximum simulated storm tide height are displayed in Table 5. The total number of accessible homes decreases as the storm tide height increases, while the total number of inaccessible homes increases. Homes in Bangalee, South Yeppoon (Cooee Bay) and northeast Rosslyn are completely inaccessible for each percentile range storm tide height. As the storm tide height increases to the maximum simulated height, more homes in Taranganba and Lammermoor become inaccessible. The flood vulnerability model is likely underestimating the number of inaccessible homes than what is presented here given that complex inland flooding was not simulated with the inclusion of flow velocity and wave effects on the buildings. Also, the method assumes slow rising waters, which have been shown to not result in major structural damage. Future research will expand the storm tide risk assessment to include these factors and a damage indicator that further determines if residents will be displaced for an extended time from their residence.

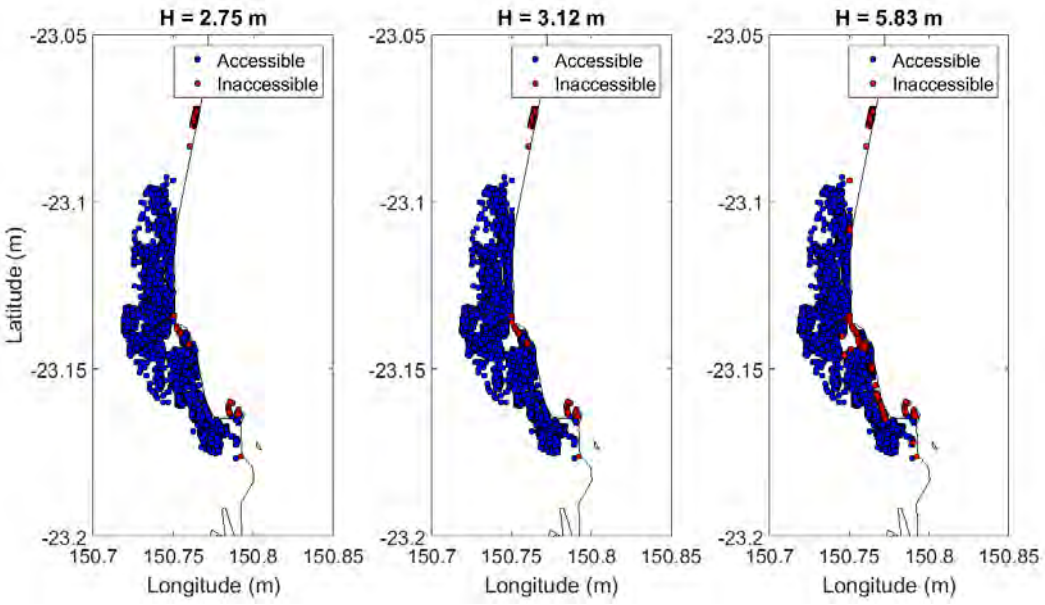

Figure 22. Accessible and inaccessible synthetic residential buildings for the 50th and 75th percentile maximum simulated storm tide heights. The maximum simulated storm tide height for the entire ensemble event set is also displayed.

Table 5. Total number of accessible and inaccessible houses based on the maximum simulated storm tide height.

Storm tide height (m)	Number of accessible buildings	Number of inaccessible buildings
2.75	9,127	167
3.12	9,119	175
5.83	8,791	503

5 CONCLUSIONS AND FUTURE RESEARCH

It is imperative that potential tropical cyclone impacts are understood prior to occurrence to mitigate the loss of life and property. Disaster scenario analysis is one method typically employed to better understand the impacts and subsequent emergency management requirements of events larger than those experienced historically. In this scenario, a modified version of the 72 hr ECMWF ensemble prediction system forecast was used to simulate fifty semi-realistic variations of Severe Tropical Cyclone Marcia (2015). Both wind and storm tide hazard footprints were generated for each simulation to examine the distribution of maximum three-second gust wind speeds and storm tide heights at landfall. The wind and storm tide hazard footprints from each simulation were ingested by wind and flood vulnerability models to assess the range of potential wind and storm tide-induced damage at building level using a G-NAF exposure dataset aggregated to match the SA1 statistics listed in NEXIS 2011. Based on the degree of wind-induced damage experienced and the storm tide inundation depth at each synthetic residential building, houses were either deemed inhabitable/uninhabitable or accessible/inaccessible. The compounding impacts of rainfall and inland flooding have been left to be explored in future research.

Consequences of the simulated wind fields and storm tides were at times catastrophic. For some of the worst-case wind and storm tide scenarios (i.e. the 10% probability of occurrence scenarios), 43% of the synthetic residential buildings would require major structural repairs due to extreme wind gusts, particularly in Byfield and Yeppoon. Residences in Yeppoon and other low-lying areas would also be exposed to high water levels (3.12 m – 5.83 m for extreme cases), which would result in significant building and contents damage. Estimates of the number of people displaced due to wind and storm tide-induced residential building damage and building level loss estimates were difficult to produce given the challenge in realistically assigning people and building values per individual dwelling (e.g. houses versus apartments) based on NEXIS 2011. When ground truth G-NAF data is released, future research will update the current building level exposure dataset to include estimates of people per dwelling, as well as, age and wealth information to determine what populations would require shelter or financial assistance during and after an event. Individual building values will also be assigned.

Future work will aim to perform the following research tasks:

- Include power lines and water distribution networks in the exposure dataset.
- Incorporate new atmospheric variables in the wind hazard model (e.g. deep layer wind shear and sea surface temperatures).
- Calibrate the rainfall model for Australian terrain and topography.
- Develop a rainfall runoff model that can be coupled with the calibrated rainfall hazard model to evaluate inland flooding impacts.
- Extend the Coral Sea mesh inland to simulate complex inland storm tide flooding.
- Update the flood vulnerability models to include flow velocity and waves.
- Update the building level exposure dataset with ground truth G-NAF data.
- Assess the impact of joint hazards (i.e. wind driven rain).

6 REFERENCES

Beaman, R. (2010). Project 3DGBR: a high-resolution depth model for the Great Barrier Reef and Coral Sea. MTSRF Final Report, Reef and Rainforest Research Centre. James Cook University.

Department of Natural Resources and Mines (2005). Digital elevation model - 25metre - Fitzroy River catchment - data package. Queensland Government Queensland Spatial Catalogue.

Egbert, G. D. and S. Y. Erofeeva (2002). "Efficient inverse modeling of barotropic ocean tides." Journal of Atmospheric and Oceanic Technology. **19**, 183 - 204.

Egorova, R., J. M. van Noortwijk, and S. R. Holterman (2008). "Uncertainty in flood damage estimation." International Journal of River Basin Management. **6**, 139 – 148.

FEMA (2009). HAZUS-MH MR4 Hurricane Model Technical Manual. Washington DC, USA.

FEMA (2013). HAZUS-MH MR4 Flood Loss Model Technical Manual. Washington DC, USA.

Geoscience Australia (2012). National Exposure Information System (NEXIS) product description for Statistical Area Level 2 (SA2) aggregated information. Canberra, Geoscience Australia.

Geoscience Australia (2014). National Dynamic Land Cover Dataset (DLCD) product description. Canberra, Geoscience Australia.

Ginger, J., D. Henderson, M. Edwards and J. Holmes (2010). Housing damage in windstorms and mitigation for Australia. 2010 APEC-WW and IG-WRDRR Joint Workshop: wind-related disaster risk reduction activities in Asia-Pacific Region and Cooperative Actions, Incheon, Korea.

Harper, B. A. and G. J. Holland (1999). An updated parametric model of the tropical cyclone. In Proceedings of the 23rd Conference on Hurricanes and Tropical Meteorology, American Meteorological Society, Dallas, Texas, 10-15 January, 1999.

Harper, B. (2001). Queensland climate change and community vulnerability to tropical cyclone: Ocean hazards assessment - stage 1. SEA Doc. No. J0004-PR001C.

Henderson, D., J. Ginger, C. Leitch, G. Boughton and D. Falck (2006). Tropical Cyclone Larry damage to buildings in the Innisfail area (Technical Report 51). Townsville, Qld, Australia, Cyclone Testing Station, James Cook University.

Holland, G. J. (1980). "An Analytic Model of the Wind and Pressure Profiles in Hurricanes." Monthly Weather Review **108**, 1212-1218.

Lin, N. and D. Chavas (2012). "On hurricane parametric wind and applications in storm surge modelling." Journal of Geophysical Research: Atmospheres. **117**, 1 - 19.

Lonfat, M., F. D. Marks, and S. Chen (2004). "Precipitation distribution in tropical cyclones using the Tropical Rainfall Measuring Mission (TRMM) Microwave Imager: A global perspective." Monthly Weather Review, **132,** 1645–1660.

Mason, M., E. Phillips, T. Okada, and J. O'Brien (2012). Analysis of damage to buildings following the 2010 - 11 Eastern Australia floods. Gold Coast, Australia. National Climate Change Adaptation Research Facility. pp. 95.

Mason, M. (2015). Year 1 scenario: A Southeast Queensland tropical cyclone scenario - wind damage and impacts. BNHCRC Report.

Mason, M. and R. J. Krupar III (2015). Year 2 scenario selection: Southeast Qld/Northern NSW tropical cyclone scenario - wind and rain-induced inundatuon and damage. BNHCRC Report.

Mason, M. and K. Parackal (2015). Vulnerability of buildings and civil infrastructure to tropical cyclones: A preliminary review of modelling approaches and literature. BNHCRC Report.

Smith, D. and D. Henderson (2015). Insurance claims data analysis for Cyclones Yasi and Larry (CTS Report: TS1004.2), Cyclone Testing Station: James Cook University.

Sparks, P. and S. Bhinderwala (1994). Relationship between residential insurance losses and wind conditions in Hurricane Andrew. Hurricanes of 1992@ sLessons Learned and Implications for the Future, ASCE.

Standards Australia (2011). AS/NZS1170.2 - Structural design actions Part 2: Wind actions. Sydney, Australia.

Simiu, E., and Scanlan, R.H. (1996). Wind effects on structures: Fundamentals and applications to design. 3rd Edition. John Wiley & Sons, New York, N.Y.

The National Aeronautics and Space Administration, Image of the Day: Cyclones Lam and Marcia, accessed 21 June 2017, <https://earthobservatory.nasa.gov/IOTD/view.php?id=85335>.

Tuleya, R. E., M. DeMaria, and J. R. Kuligowski (2007). "Evaluation of GFDL and simple statistical model rainfall forecasts for U.S. landfalling tropical storms." Weather and Forecasting, **22,** 56–70.

Vickery, P. J. (2005). "Simple Empirical Models for Estimating the Increase in the Central Pressure of Tropical Cyclones after Landfall along the Coastline of the United States." Journal of Applied Meteorology **44**, 1807-1826.

Vickery, P. J. and D. Wadhera (2008). "Statistical models of Holland pressure profile parameter and radius to maximum winds of hurricanes from flight-level pressure and H*Wind data." Journal of Applied Meteorology and Climatology **47**, 2497-2517.

Walker, G. (1995). "Wind vulnerability curves for Queensland houses." Alexander Howden Reinsurance Brokers (Australia) Ltd., Sydney.

Wieringa, J. (1992). ‘’Updating the Davenport roughness classification.’’ Journal of Wind Engineering and Industrial Aerodynamics **41**, 357-368.

Whiteway, T. G. (2009). Australian bathymetry and topography data. Canberra, Geoscience Australia.

Yang, T. (2016). Wind multiplier dataset product description. Canberra, Geoscience Australia.

7 APPENDIX A

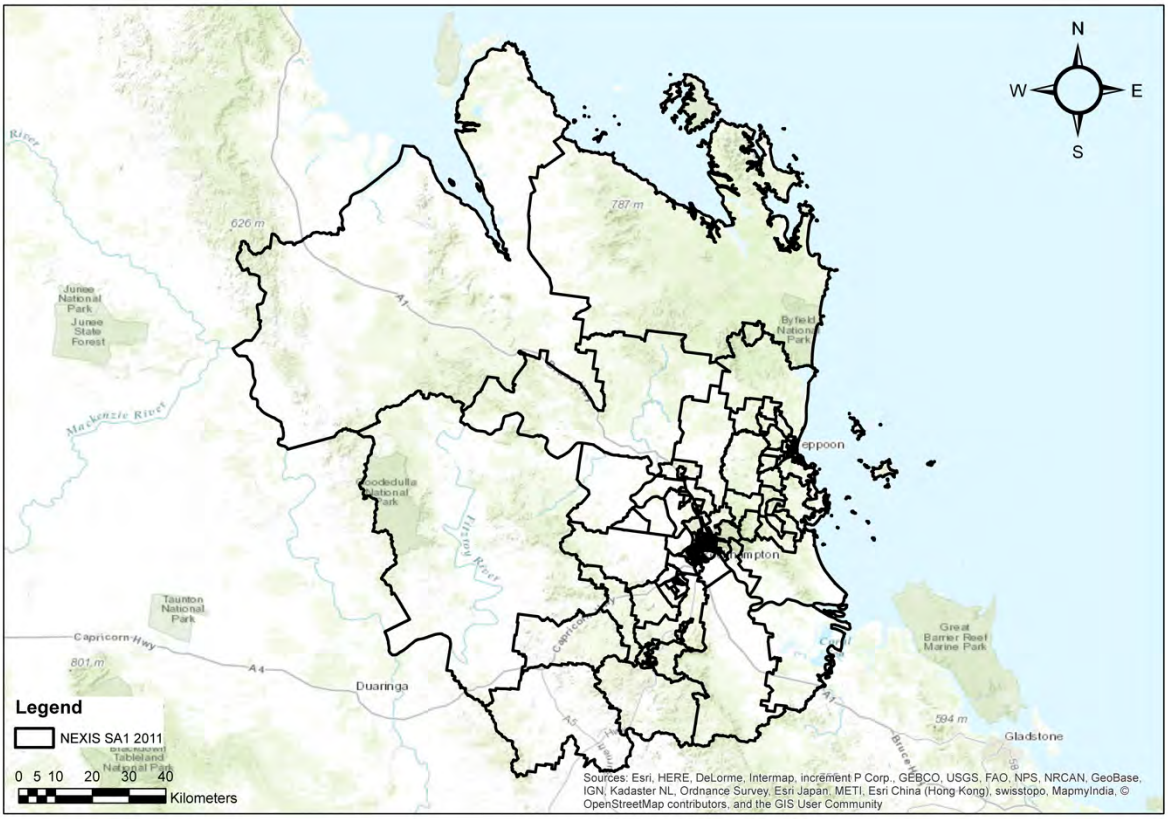

Figure A1. NEXIS SA1 boundaries used to generate the synthetic building exposure dataset.